Rainbow Enhanced Elastic Scattering of Gaussian Beams from Microspheres in Infrared Wavelengths

by

Onur Akatlar

A Thesis Submitted to the
Graduate School of Engineering
in Partial Fulfillment of the Requirements for
the Degree of

Master of Science
in
Material Science and Engineering

Koç University

September 2006

Koç University

Graduate School of Sciences and Engineering

This is to certify that I have examined this copy of a master's thesis by

Onur Akatlar

and have found that it is complete and satisfactory in all respects,
and that any and all revisions required by the final
examining committee have been made.

Committee Members:

_____

Ali Serpengüzel, Ph. D. (Advisor)

_____

Özgür Müstecaplıoğlu, Ph. D.

_____

Erdem Alaca, Ph. D.

Date: _____

ABSTRACT

Microspheres are utilized for various applications in optoelectronics owing to their high quality factor cavity resonances that are called morphology dependent resonances (MDR's) or whispering gallery modes (WGM's). Among these applications are biodetectors, ultrafine sensors, rotation sensors and wavelength division multiplexing components such as microlasers, optical couplers, optical filters, modulators, and channel droppers. In this work, we calculate the intensity of elastic scattering of an electromagnetic wave from a microsphere for transverse electric and transverse magnetic polarizations. Calculations are performed for Gaussian beams. We specifically calculate the rainbow enhanced elastic scattering intensity for Gaussian beams by using the localization principle and Generalized Lorenz Mie Theory. Three spectral ranges are studied : Near-infrared (1530 nm to 1570 nm), mid-infrared (10.4 μm to 10.8 μm) and far-infrared (95 μm to 100 μm). In each of the spectral ranges, we used microspheres having different refractive indices of 2, 1.4142, 1.236, and 1.15. The maximum elastic scattering efficiencies at near infrared, mid-infrared and far-infrared ranges are calculated to be 11%, 8%, and 7%, respectively, provided that appropriate impact parameters are used. Potential materials are found to be lithium fluoride (m = 1.4142 @ 1550 nm), silicon monoxide (m = 2 @ 10 μm), lithium niobate (m = 1.236 @ 10 μm), lead telluride (m = 2 @ 100 μm), potassium chloride (m = 1.4142 @ 100 μm) and lead selenide (m = 1.15 @ 100 μm). These materials are transparent at the quoted spectral bands and are amenable to optoelectronic device applications.

ÖZET

Mikroküreler, yüksek kalite faktörüne sahip yapısal çınlamaları sayesinde çeşitli optoelektronik cihaz uygulamalarında kullanılırlar. Biyodedektörler, ve hassas algılayıcıların yanı sıra mikrolazerler, optik bağlaştırıcılar, optik filtreler, ve kanal düşürücüler gibi dalgaboyu bölmeli, çoklama elemanları da bu uygulamalar arasında sayılabilir. Bu çalışmada, enine manyetik ve enine elektrik polarizasyonlu elektromanyetik dalga için mikroküreden elastik saçılma yoğunluğunu hesapladık. Hesaplamalar Gauss ışınları için gerçekleştirildi. Özellikle, lokalizasyon prensibi ve genelleştirilmiş Lorenz Mie Teorisi kullanarak gauss ışınları için gökkuşağı tarafından yükseltilmiş elastik saçılmalar hesaplandı, üç ışık tayfı bandı üzerinde çalışıldı: Yakın-kızılötesi (1530 nm'den 1570 nm'ye), orta-kızılötesi(10.4 μm'den 10.8 μm'ye) ve uzak-kızılötesi (95 μm'den 100 μm'ye). Her bir ışık tayfı bandında, kırılma indisleri, 2, 1.4142, 1.236, ve 1.15 olan mikroküreler kullandıldı. Yakın-kızılötesi, orta-kızılötesi ve uzak-kızılötesi bandlarında maksimum saçılma verimleri sırasıyla %11, %8, ve %7 olarak hesaplandı. Bu bandlarda potansiyel malzemeler, lityum florür (m = 1.4142 @ 1550 nm), silikon monoksit (m = 2 @ 10 μm), lityum niyobat (m = 1.236 @ 10 μm), kurşun tellürür (m = 2 @ 100 μm), potasyum klorür (m = 1.4142 @ 100 μm) ve kurşun selenid (m = 1.15 @ 100 μm). Bu malzemeler, yukarıda adı geçen tayf bandlarında transparandırlar ve optoelektronik cihaz uygulamalarına uygundurlar.

ACKNOWLEDGEMENTS

I would like to thank to my advisor Professor Ali Serpengüzel for the guidance he has provied me during my graduate study at the Koç University Microphotonics Research Laboratory (KUMRL). I also would like to thank Adnan Kurt for providing me guidance and support in (KUMRL). I would like to thank Professor James Lock for providing me theoretical and numerical support for the Gaussian beam calculations. I want to thank Professor Özgür Müstecaplıoğlu and Professor Erdem Alaca for providing me constructive feedback about my thesis research. I would like to thank to my friends at KUMRL Ulas Kemal Ayaz and Sinan Fındık for their friendship. Last but not the least, I would like to thank my father Mustafa Akatlar, my mother Handan Akatlar, my sister Pınar Akatlar, and my fiancé Hilal Aytas for providing me a peaceful environment for developping my thesis work. I wish to dedicate my thesis to my family.

TABLE OF CONTENTS

List of Figures viii

Nomenclature xi

Chapter 1: Introduction 1

Chapter 2: Microsphere Resonator and Morphology Dependent Resonances 3

2.1 Microsphere Resonator. 3
2.2 Lorenz Mie Theory 4
2.3 Q-Factor of Morphology Dependent Resonances. 7
2.4 Mode Spacing 8
2.5 Generalized Lorenz Mie Theory. 9
2.6 Excitation of Morphology Dependent Resonances.. 10

Chapter 3: Rainbows and Gaussian Beam Excitation of MDRs 12

3.1 Rainbows 12
3.1.1 Ray Optics Interpretation of Rainbow Formation 13
3.1.2 Periodic Rainbows 14
3.3 Gaussian Beam Excitation of MDRs and Geometry of Numeric Calculations . . 16

Chapter 4: Rainbow Enhanced Scattering in Near Infrared Wavelengths 19

4.1 Introduction. 19
4.2 Calculations and analysis. 19

Chapter 5: Rainbow Enhanced Scattering in Mid Infrared Wavelengths 26

5.1 Introduction. 26
5.2 Calculations and analysis. 26

Chapter 6: Rainbow Enhanced Scattering in Far Infrared Wavelengths 33

6.1 Introduction. 33
6.2 Calculations and analysis. 33

Chapter 7: Conclusion 40

Bibliography 42

Vita 47

LIST OF FIGURES

Figure 2.1 Total internal reflections on the interior surface of the microsphere……4

Figure 2.2 Illustration of internal intensity distribution for n = 12, l = 2…….……..5

Figure 2.3 Illustration of a single MDR…….…….7

Figure 2.4 Expected MDR spectra with four consecutive modes……...8

Figure 2.5 Geometry of efficiency calculation…….....11

Figure 3.1 Illustration of scattering of two rays from a sphere……13

Figure 3.2 Three periodic reflections in a sphere…….. . . . . … 14

Figure 3.3 Image of periodic rainbow reflections…….15

Figure 3.4 Geometry of calculations for MDR and rainbow phases……17

Figure 3.5 Illustration of Gaussian beam illumination…….16

Figure 3.6 Geometry of numeric calculations…….....17

Figure 3.7 Geometry of (a) TE (b) TM calculations…….18

Figure 4.1 False color elastic scattering intensity of (a) transverse electric (TE)
(b) transverse magnetic (TM) polarized Gaussian beam from a microsphere
of radius a = 10 μm, refractive index m = 2, and rainbow order p =3……..……21

Figure 4.2 False color elastic scattering intensity of (a) transverse electric (TE)
(b) transverse magnetic (TM) polarized Gaussian beam from a microsphere
of radius a = 10 μm, refractive index m = 1.4142, and rainbow order p =4 ……..…..22

Figure 4.3 False color elastic scattering intensity of (a) transverse electric (TE)
(b) transverse magnetic (TM) polarized Gaussian beam from a microsphere
of radius a = 10 μm, refractive index m = 1.236, and rainbow order p =5 ……..…24

Figure 4.4 False color elastic scattering intensity of (a) transverse electric (TE)
(b) transverse magnetic (TM) polarized Gaussian beam from a microsphere
of radius a = 10 μm, refractive index m = 1.15, and rainbow order p =6……..…...25

Figure 5.1 False color elastic scattering intensity of (a) transverse electric (TE)
(b) transverse magnetic (TM) polarized Gaussian beam from a microsphere
of radius a = 100 μm, refractive index m = 2, and rainbow order p =3 ……...28

Figure 5.2 False color elastic scattering intensity of (a) transverse electric (TE)
(b) transverse magnetic (TM) polarized Gaussian beam from a microsphere
of radius a = 100 μm, refractive index m = 1.4142, and rainbow order p =4……...29

Figure 5.3 False color elastic scattering intensity of (a) transverse electric (TE)
(b) transverse magnetic (TM) polarized Gaussian beam from a microsphere
of radius a = 100 μm, refractive index m = 1.236, and rainbow order p =5…….....31

Figure 5.4 False color elastic scattering intensity of (a) transverse electric (TE)
(b) transverse magnetic (TM) polarized Gaussian beam from a microsphere
of radius a = 100 μm, refractive index m = 1.15, and rainbow order p = 6 ……..…...…32

Figure 6.1 False color elastic scattering intensity of (a) transverse electric (TE)
(b) transverse magnetic (TM) polarized Gaussian beam from a microsphere
of radius a = 500 μm, refractive index m = 2, and rainbow order p = 3 ……..…34

Figure 6.2 False color elastic scattering intensity of (a) transverse electric (TE)
(b) transverse magnetic (TM) polarized Gaussian beam from a microsphere
of radius a = 500 μm, refractive index m = 1.4142, and rainbow order p =4 ……..……....36

Figure 6.3 False color elastic scattering intensity of (a) transverse electric (TE)
(b) transverse magnetic (TM) polarized Gaussian beam from a microsphere
of radius a = 500 μm, refractive index m = 1.236, and rainbow order p = 5……...…38

Figure 6.4 False color elastic scattering intensity of (a) transverse electric (TE)
(b) transverse magnetic (TM) polarized Gaussian beam from a microsphere
of radius a = 500 μm, refractive index m = 1.15, and rainbow order p = 6……..…39

NOMENCLATURE

a	Microsphere radius
a_n	Elastically scattered transverse magnetic field coefficient
b_n	Elastically scattered transverse electric field coefficient
a_{nm}	Partial wave coefficient for transverse magnetic field
b_{nm}	Partial wave coefficient for transverse electric field
$\Delta\lambda$	Mode spacing in wavelength
$\delta\lambda$	Wavelength shift
$\Delta\theta_R$	Spread Angle
ϵ	Permittivity of the medium
ϵ	Energy in a resonance mode
$h_n^1(x)$	Spherical Hankel function of the first kind
$h_n^2(x)$	Spherical Hankel function of the second kind
$H_r(\Omega)$	Radial component of magnetic field
$j_n(x)$	Spherical Bessel function
K	Imaginary part of refractive index
l	Mode order
λ	Wavelength of light in vacuum
m	Azimuthal mode number
m	Real part of refractive index
μ	Permeability of the medium

n	Complex refractive index
n	Polar mode number
n_R	Rainbow order
P_i	Power coupled into a MDR
$\psi_n(x)$	Ricatti Bessel Function
Q	Quality factor of a MDR
σ_{MDR}	Scattering cross section of a mode
σ_{total}	Total scattering cross section
τ	Average lifetime of photons
θ_i	Angle of incidence
ω_o	Half width of Gaussian beam
ω	Optical angular freqeuncy
x	Size parameter of the microsphere
$Y_{nm}^*(\Omega)$	Spherical harmonic function

Chapter 1

INTRODUCTION

Various kinds of optical resonators are utilized in optics and optoelectronics for linear and nonlinear applications. One of the characteristic properties of the resonators is the quality factor (Q-factor). Quality factor is the numeric value that provides a quantitative description of the sharpness of the peak, and the relative amount of energy trapped in the resonator. An appropriate resonator for an application is determined by examining the needs of the application and the quality factor that is necessary for the application. There are several kinds of resonators with different properties and Q-factors. Fabry-Perot resonators [1,2], microring resonators [3], and microsphere resonators [4] are some of the well known and used resonator types in optics and optoelectronics. Microspheres have high resolving performance thanks to their high quality factor morphology dependent resonances (MDR), i.e., whispering gallery modes (WGM) [5,6]. Quality factors on the order of 10^{10} are reported [7] from microspheres. Microspheres are utilized in various applications including wavelength division multiplexing (WDM) applications such as channel dropping filters [8], optical switches [9], ultrafine sensors [10], displacement sensors [11], and rotation detectors [12]. All of the above applications require high quality factor whispering gallery modes (WGM's). Elastic scattering properties of a microsphere should be studied out before utilizing the microsphere as an optical component. The properties of elastic scattering can be determined experimentally or numerically. We determined the elastic scattering properties, such as mode spacing (analogue of free spectral range (FSR) in a Fabry-Perot resonator) of consecutive MDR's, quality factor of resonances, and excitation efficiency, numerically by calculating the elastic scattering of a

Gaussian beam from a microsphere. Off- axis Gaussian beam illumination of a microsphere results in higher coupling efficiency [13] when compared with plane wave illumination. We concentrated on the elastic scattering of transverse electric (TE) and transverse magnetic (TM) fields that are focused as a Gaussian beam with an appropriate impact parameter (b). The calculations are based on Generalized Lorenz Mie Theory (GLMT) [13]. Additionally, we concentrated on periodic rainbow formations in order to determine, whether there is elastic scattering enhancement due to rainbows.

We have calculated the elastic scattering intensities from microspheres of different refractive indices that correspond to periodic rainbow formations. The calculations are performed for refractive indices of m= 2, 1.4142, 1.236, and 1.15. Three spectral ranges are selected for different applications. For the near-infrared, the range between 1530 nm to 1570 nm, the conventional (C) band is considered. For mid-IR range, wavelengths between 10.4 μm to 10.8μm are considered for atmospheric applications, since the atmosphere has very little absorption at 10 μm. Far-IR calculations are performed between wavelengths of 95 μm to 100 μm. This range is considered for only space based applications due to high atmospheric absorption at these wavelengths.

Chapter 2 includes information about microspheres, as well as a description of the morphology dependent resonances (MDR's). Chapter 3 describes the MDR's of a microsphere using Generalized Lorenz Mie Theory (GLMT) using a Gaussian beam. Chapter 3 discusses the relative phase between the MDRs and the rainbows. Chapter 4 presents the calculated spectrum at near-IR range (C-band) between wavelengths 1530 nm to 1570 nm. Chapter 5 reveals elastic scattering properties of microspheres with different refractive indices in the mid–IR range. Chapter 6 is about elastic scattering properties of microspheres at far-IR wavelengths between 95 μm and 100 μm. Chapter 7 is the conclusion, and discusses the factors affecting the rainbow enhancement of the MDRs. The thesis is concluded with the presentation of the potential optoelectronic materials for future experimental studies.

Chapter 2

MICROSPHERE RESONATORS AND MORPHOLOGY DEPENDENT RESONANCES

2.1 Microsphere Resonators

In the beginning of 19th century, Gustav Mie suggested the existence of modes in a dielectric spherical particle in the context of light scattering from spherical particles. The spectrum has sharp peaks owing to the resonance of light confined in the microsphere. The confinement happens because of almost total internal reflections (TIR's) at the dielectric surface of the spherical particle. These modes are generally called whispering gallery modes (WGM's). The term, whispering gallery modes refers to the article of Lord Rayleigh that is published in 1912, describing the propagating acoustic waves around the gallery of Saint Paul's Cathedral in London [14]. A whisper that is close to the walls of the circular gallery of the cathedral can travel to the other side.

The formation of WGM's or morphology dependent resonances (MDR's) can be described by ray optics. Once a ray enters the microsphere and intersects the inner surface of the dielectric sphere beyond the critical angle, it is totally reflected [15]. Figure 2.1 shows that the total internal reflections propagate on a circular optical path remaining confined in a thin layer under the surface [16]. If the optical path length of the reflections is equal to an integer multiple of wavelength, the rays return to initial position in phase [17] and constructively interfere. The constructive interference is wavelength and size dependent [18]. Wave optics introduce MDR's as standing waves on the internal wall of the microsphere but ray optics can not provide sufficient description about the coupling of the waves. The quantum mechanical approach suggests that the microsphere stands in a

potential well [19], energy is trapped near the surface, and coupling is due to tunneling through the outer wall of the potential well.

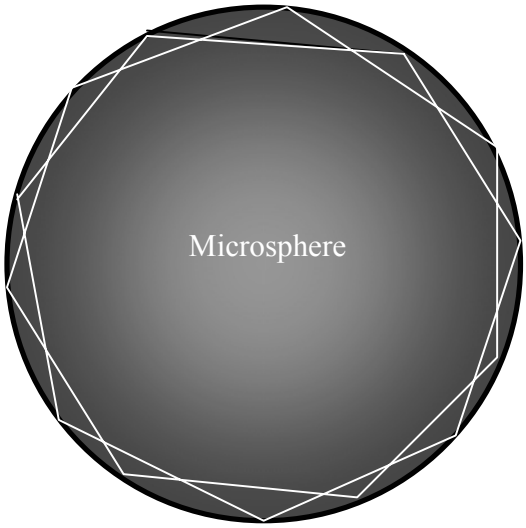

Figure 2.1 Total internal reflections on the interior surface of the microsphere.

2.2 Lorenz Mie Theory

Lorenz Mie theory explains light scattering from spherical particles. German physicist Gustav Mie and Danish physicist Ludvic Lorenz developed the theory of light scattering from a dielectric sphere in 1908 [20]. The theory is about the illumination by a plane wave of a homogenous isotropic and optically linear material. In this theory the incident plane wave is expanded into vector spherical harmonics. The field is expanded into vector Spherical harmonics and by applying the boundary conditions on the spherical surface, the expansion coefficients of the scattered field are computed.

MDR's occur at discrete wavelengths and depend on the size parameter (x) and refractive index of the microsphere. MDR's are defined by three mode numbers: Azimuthal mode number (*m*), polar mode number (*n*), and radial mode number (*l*) [21]. Polar mode number (*n*) defines the number of maxima on the internal surface of the sphere. Radial mode number (*l*) defines the number of maxima in the radial direction (on the radius) of the sphere. Figure 2.2 explains the polar and radial mode numbers and illustrates the shape of the modes.

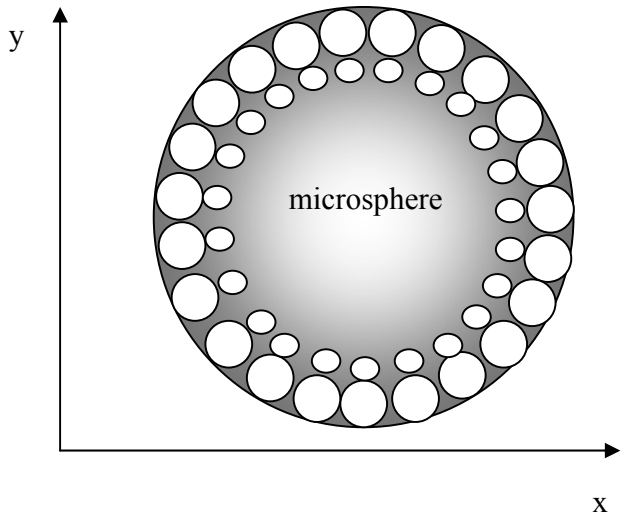

Figure 2.2 Illustration of internal intensity distribution for $n = 12$, $l = 2$ mode.

Polarization of electromagnetic field is also effective on characteristics of the MDR's. MDR's can be identified by mode numbers and polarization of the mode: transverse electric (TE) and transverse magnetic (TM). The electromagnetic fields on the dielectric medium surface obey Eq.2.1 and Eq.2.2 [22].

$$\frac{\left[mxj_n(mx)\right]'}{j_n(mx)} = \frac{\left[xh_n^{(1)}(x)\right]'}{h_n^{(1)}(x)} \qquad (2.1),$$

$$\frac{[mj_n(mx)]'}{m^2 j_n(mx)} = \frac{[xh_n^{(1)}(x)]'}{h_n^{(1)}(x)} \quad (2.2),$$

and where x = 2πa/λ is the size parameter, a the radius of the sphere and, λ the wavelength in vacuum, m the refractive index, $j_n(x)$ the first kind spherical Bessel function, and $h_n^{(1)}(x)$ is the first kind spherical Hankel function [22]. The coefficients of elastically scattered transverse magnetic (TM) and transverse electric (TE) fields are (a_n) and (b_n) respectively, in Eq.2.3 and Eq.2.4. $h_n^{(2)}$ is a Hankel function of the second kind.

$$a_n = \frac{j_n(x)[mxj_n(mx)]' - m^2 j_n(mx)[xj_n(x)]'}{h_n^{(2)}(x)[mxj_n(mx)]' - m^2 j_n(mx)[xh_n^{(2)}(x)]'} \quad (2.3),$$

$$b_n = \frac{j_n(x)[mxj_n(mx)]' - j_n(mx)[xj_n(x)]'}{h_n^{(2)}(x)[mxj_n(mx)]' - j_n(mx)[xh_n^{(2)}(x)]'} \quad (2.4).$$

The prime stands for the derivative with respect to the argument [23]. The MDRs of a microsphere are observed for the wavelengths that makes the denominators of a_n and b_n coefficients zero, in other words in the poles of coefficient equations [24]. The resonances are not at a single discrete wavelength. They occur for every pole of the coefficients a_n and b_n [27]. Each pole starting from the smallest value defines resonances starting from first order. The polar mode number (n) of MDRs can take values $x \leqslant n \leqslant mx$ [26].

2.3 Q-Factor of Morphology Dependent Resonances

Main properties of the MDR's are quality factor (Q), mode spacing, and mode position. Quality factor (Q) can be defined as the ratio of the energy of confined photons to the energy of escaped photons during one circular trip. Q-factor determines how long a photon

stays in the MDR. Q = $\omega\tau$, where τ stands for the average life time of photons and ω stands for the angular frequency [27]. Another definition regarding Q factor is $\lambda_{n,l}/\delta\lambda$ where $\lambda_{n,l}$ stands for position (wavelength) of the MDR and $\delta\lambda$ stands for full width at half maximum (FWHM) of the related resonance. Figure 2.3 illustrates an MDR and describes the Q factor. Angular mode number (n) and radial mode number (l) effect on the quality factor of the resonance. Resonances closer to the surface have lower volume, and have higher Q factors [28]. As n increases the Q factor also increases. Highest Q-factors belong to lowest radial mode number (l) and highest polar mode number (n).

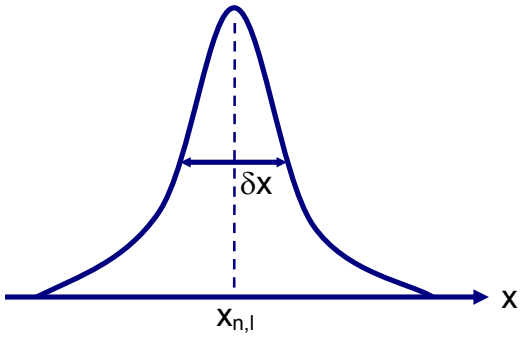

Figure 2.3 Illustration of a single MDR spectrum.

2.4 Mode Spacing

Mode spacing may have various meanings when different angular mode number (n) and radial mode number (l) combinations are considered. By "Mode Spacing", we mean the spacing between subsequent angular mode numbers (n) but same radial mode number (l). The relation is given by Eq.2.5 and illustrated by the figure 2.4 [29]. m is the refractive index of the microsphere and a is the radius of the microsphere.

$$\Delta\lambda_{n,l} = \lambda_{n+1,l} - \lambda_{n,l} = \frac{\lambda^2}{2\pi a}\frac{\tan^{-1}(\sqrt{m^2-1})}{\sqrt{m^2-1}} \tag{2.5}$$

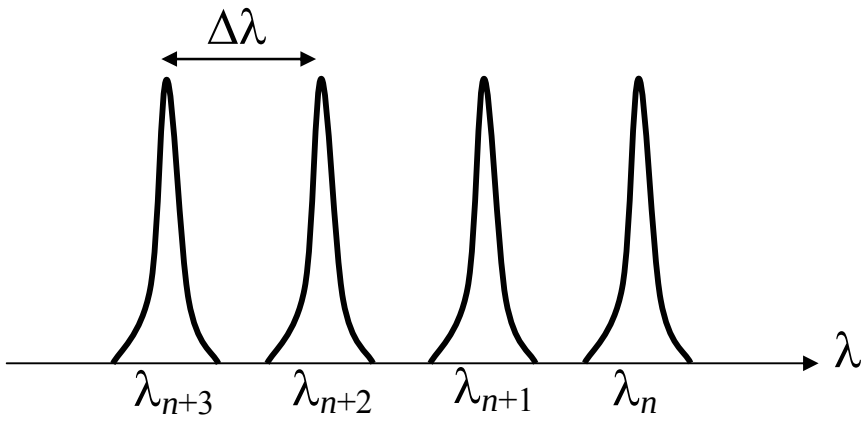

Figure 2.4 Expected MDR spectra with four consecutive mode numbers (*n*) for a given mode order (*l*)

2.5 Generalized Lorenz Mie Theory

Lorenz Mie theory explains the elastic scattering of plane wave from an isotropic spherical particle. But experimental observations suggest an enhancement due to focused Gaussian beam excitation of MDRs of the spherical particle. A generalization of the Lorenz Mie theory which is called Generalized Lorenz Mie theory (GLMT) has been developed. Generalized Lorenz Mie theory, removes the waves that has angular momentum quantum number (*n*) smaller than size parameter ($x = 2\pi a/\lambda$) from the infinite series of Lorenz Mie theory [30]. The angular momentum quantum number (*n*) that is necessary for interacting with the microsphere surface according to Lorenz Mie theory has to satisfy $mx \geq n \geq x$.

m is the relative refractive index (refractive index of microsphere / refractive index of medium). By applying the localization principle this inequality turns to be ma ⩾ b ⩾ a. Thus a ray with an impact parameter (b) satisfying the inequality can excite MDRs of the microspheres.

In GLMT the a_n and b_n coefficients for TM and TE fields in Lorenz Mie theory are replaced with a_{nm} and b_{nm} coefficients for TM and TE fields, respectively [30]. Eq.2.6 and Eq.2.7 explains the relation between b_n and b_{nm}.

$$b_{nm} = b_n B_n^m \tag{2.6},$$

$$B_n^m = \frac{a^2}{n(n+1)\psi_n(x)} \int_0^{4\pi} d\Omega H_r(\Omega) Y_{nm}^*(\Omega) \tag{2.7},$$

where $\psi_n(x)$ is the Ricatti-Bessel function, $Y_{nm}^*(\Omega)$ is the spherical function, and $H_r(\Omega)$ is the radial component of magnetic field incident on the sphere surface [30].

2.6 Excitation of Morphology Dependent Resonances (MDRs)

Plane wave excitation and focused Gaussian beam excitation of MDRs are two possible excitation methods. The difference between them is the excitation efficiency. For an MDR, power coupling into a mode is defined in Eq.2.8,

$$\frac{d\varepsilon}{dt} = \overline{\sigma_{MDR}} P_i - \frac{\varepsilon}{\tau} \tag{2.8}$$

Eq.2.9 shows the scattering cross section ratio of the MDR cross section to the total scattering cross section,

$$\overline{\sigma_{MDR}} = \frac{\sigma_{MDR}}{\sigma_{total}} \tag{2.9}$$

ϵ stands for energy in the mode, and P_i is the power incident on the microsphere. At a certain energy level, the incoming and exiting photons come to an equilibrium level, where the power coupling to a mode no longer increases. Hence by equating Eq.2.8 to zero and substituting Eq.2.9 to Eq.2.8, we obtain Eq.2.10 as *illustrated* below,

$$\varepsilon_o = \frac{\sigma_{MDR}}{\sigma_{total}} P_i \tau = \overline{\sigma_{MDR}} P_i \tau \qquad (2.10),$$

where σ_{MDR} and σ_{total} are standing for the scattering cross sections of the MDR and total scattering cross sections. For a plane wave scattered from a microsphere of radius a, the total scattering cross section is $2\pi a^2$. For a Gaussian beam the scattering cross section is $\pi w_o^2/2$. From Eq.2.10 we can conclude that, if the plane wave and Gaussian wave have the same illumination power P_i, the average energy confined in a mode is higher for a Gaussian beam due to the fact that total scattering cross section is lower. Thus excitation of MDRs of microsphere with a Gaussian beam is more efficient. The efficiency may be described from a geometric point of view for a Gaussian beam. Figure 2.5 depicts the excitation geometry.

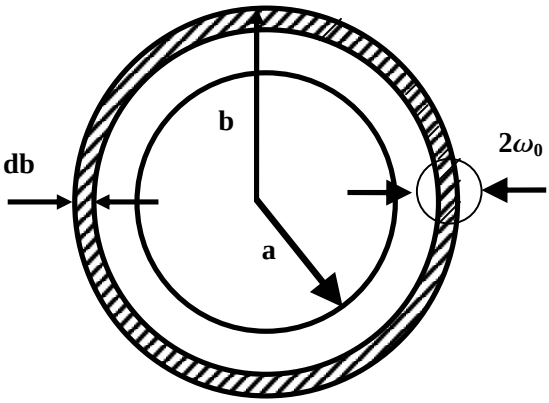

Figure 2.5 Geometry of the elastic scattering efficiency calculation.

The shaded area (σ_{MDR}) is equal to 2πbdb, where $b_n = n/k$, and hence db = 1/k. So $\sigma_{MDR} = 2\pi b/k$. Similarly the total scattering cross section is the circular area excited by a Gaussian beam is $\sigma_{total} = \pi\omega_0^2$. We substitute these equalities to Eq.2.9 and derived Eq.2.11 as follows,

$$\overline{\sigma_{MDR\ Gaussian}} \approx \sqrt{2}\lambda / \pi^2 \omega_0 \qquad (2.11).$$

Figure 2.5 depicts that the σ_{MDR} is a monotonically increasing function of (b) impact parameter. Similarly impact parameter (b) is a monotonically increasing function of polar mode number (n), (angular momentum quantum number). Therefore resonances that have higher polar mode number (n) have bigger scattering cross sections (σ_{MDR}). Eq.2.10 depicts that energy is directly proportional to scattering cross section of the mode (σ_{MDR}). This relation helps us to conclude that the higher polar mode number resonances have higher confined energy resulting in higher scattering intensity.

Chapter 3

RAINBOWS AND GAUSSIAN BEAM EXCITATION OF MDRs

3.1 Rainbows

Rainbows had been a mysterious physical phenomenan until they were first explained by Descartes in 1637 [31]. The description did not include information about color formation. An advanced theory that also includes information about color formation was suggested by Newton in 1667 [31]. The brightness of light forming rainbow is higher than the surrounding medium. Enhancement of scattered field intensity is due to rainbow glory [32]. It is important to know the basics of refraction and reflection of rays from a microsphere surface to understand physical phenomena lying beneath rainbow formation. So we will first look at the ray optics picture of rainbow formation.

3.1.1 Ray Optics Interpretation of Rainbow Formation

A ray intersecting the surface of the sphere with θ_i gets refracted with an angle θ_t satisfying the Snell's law,

$$\sin\theta_i = m\sin\theta_t \tag{3.1}$$

The refracted ray enters the sphere with angle θ_t. After p-1 total internal reflections, angle of rotation of the ray is,

$$\theta = [(p-1)\pi + 2(\theta_i - p\theta)_t] - 2N\pi \tag{3.2}$$

There is no contribution of size parameter to the equation, N is an integer. The angle only depends on the refractive index of the sphere and the incidence angle θ_i [33]. The two equations (3.1) and (3.2) describe a relation between incoming ray angle (θ_i) and angle of scattered rays after p internal reflection θ_t. If a single ray is used to illuminate the sphere, above equations suggest a single scattering angle. If several rays are incident on

microsphere surface with different angle of incidences, then each will have a different scattering angle forming a rainbow that is illustrated in figure 3.2 [34].

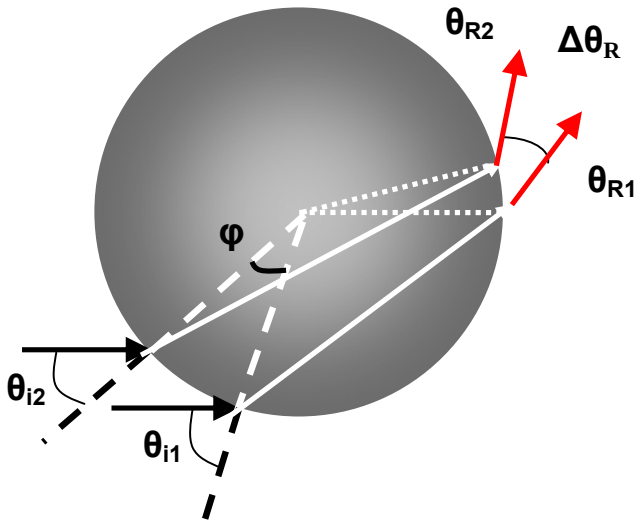

Figure 3.1 Illustration of scattering of two rays from a sphere.

The difference between θ_{R1} and θ_{R2} is the ($\Delta\theta_R$) spread angle, geometrically calculated by using the equation sequence below [35],

$$\Delta\theta_R = \theta_{R1} - \theta_{R2} \quad (3.3),$$

$$\theta_{R1} = \pi p - 2p\theta_{t1} \quad (3.4),$$

$$\theta_{R2} = \pi p - 2\varphi - 2p\theta_{t1} \quad (3.5),$$

$$\theta_{t1} = \sin^{-1}(1/m) \quad (3.6),$$

$$\theta_{t2} = \sin^{-1}\left[\frac{\sin(\pi/2-\varphi)}{m}\right] = \sin^{-1}\left(\frac{\cos\varphi}{m}\right) \quad (3.7),$$

$$\theta_{R2} = p\pi - 2\varphi - 2p\sin^{-1}\left(\frac{\cos\varphi}{m}\right) \quad (3.8).$$

By substituting Eq.3.4 and Eq.3.5 into Eq.3.3, and then substituting the Eq.3.6 and Eq.3.7 to the resulting equation, it is found that spread angle is [34],

$$\Delta\theta_R = 2\varphi - 2p\left[\sin^{-1}\left(\frac{1}{m}\right) - \sin^{-1}\left(\frac{\cos\varphi}{m}\right)\right] \tag{3.9}.$$

The spread angle is a function of refractive index *m*, which is wavelength dependent, in other words different colors (wavelengths) are diffracted at different amounts, that's why in rainbows, different colors of sunlight are seen as color bands.

3.1.2 Periodic Rainbows

If a ray which is reflected from the inner surface of the microsphere does not come to its initial position after revolving around the microsphere then in the next revolution, the ray will be reflected by a different point on the internal surface of the microsphere. Every revolution ends on a different point on the microsphere resulting in infinitely many reflection points, hence rainbow angles. In order to investigate the enhancement in scattering intensity due to rainbow formation, we work on finite number of rainbows for which we can predict the deflection angle.

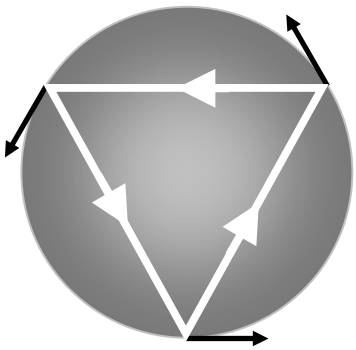

Figure 3.2 Three periodic reflections (n_R =3) in a sphere.

If a ray refracted into the sphere, return to its initial position after internal reflections as it is shown in figure 3.2, then a finite number of rainbows form since the ray will follow the same path in following reflections [34]. We call number of internal reflections, as number of rainbow angles (n_R). For periodicity of the rainbows, relationship between refractive index and number of rainbow angles is given below [34],

$$m = \frac{1}{\sin\left(\frac{\pi}{2}\frac{(n_R - 2)}{n_R}\right)}, \qquad n_R = 3,4,5,\ldots \tag{3.10}$$

Where *m* is the refractive index and p is the number of rainbows. By using Eq.3.10, refractive indices for n_R = 3, 4, 5, and 6, (as shown in Fig.3.3), are calculated to be m =2, 1.4142, 1.236, and 1.15 respectively,

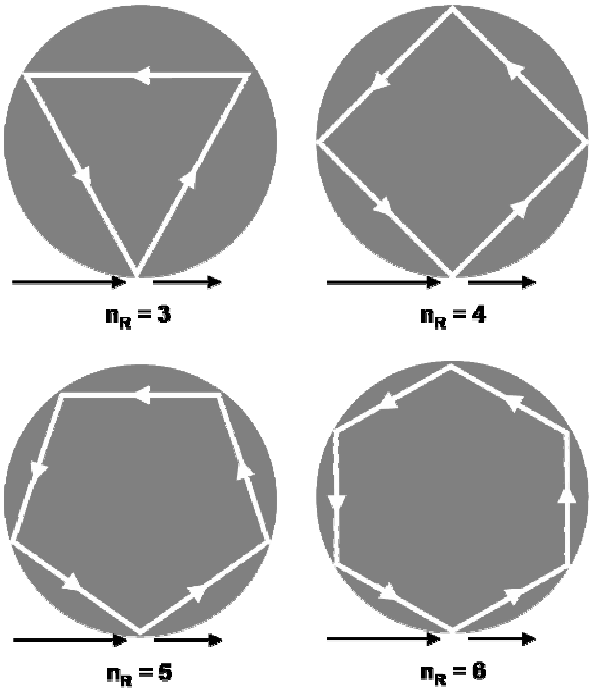

Figure 3.3 Periodic rainbow reflections for n_R = 3, 4, 5, 6.

3.3 Gaussian Beam Excitation of MDRs and Geometry of Numeric Calculations

We have calculated the elastic scattering intensity from microspheres. Elastic scattering means there is no energy loss because of scattering. Optical properties of materials are defined by complex refractive index,

$$n = m + iK \tag{3.11}$$

where n is the complex refractive index, m the real, and K the imaginary part of the complex refractive index. The imaginary part is related with absorption and real part is related with refraction. Hence we calculated scattering intensities for microspheres made of materials with negligeable K. Refractive index is a function of electrical permittivity (ϵ) and magnetic permeability (μ) of the material and also a function of wavelength. We have calculated elastic scattering intensities in three spectral ranges. Then we searched for a material that has corresponding values for each refractive index and spectral range pair. The material is required to have desired m and negligeable K ($K \ll 1$). Figure 3.5 shows the Gaussian beam illumination of a sphere,

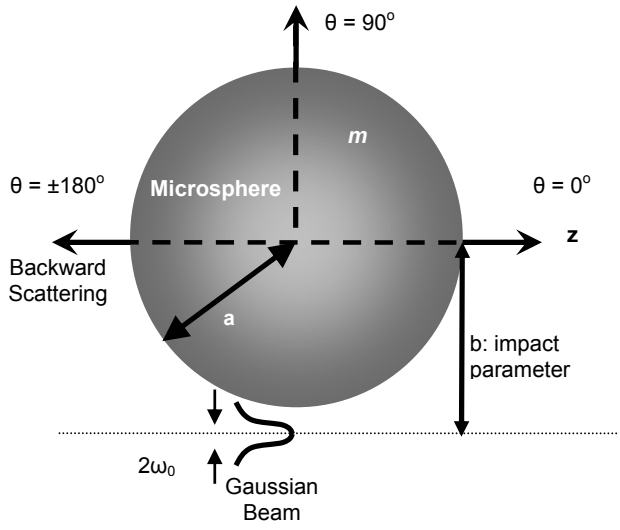

Figure 3.5 Illustration of the Gaussian beam illumination.

where ω_o is the half width of the Gaussian beam, b the impact parameter, a the radius and *m* the real part of refractive index.

Figure 3.6 illustrates the geometry for numeric calculations. The polarization of the electric field of the electromagnetic wave is always in the X direction. The Poynting vector of the wave is in the +Z direction. We have calculated the elastic scattering of Gaussian beam for both TE and TM polarizations.

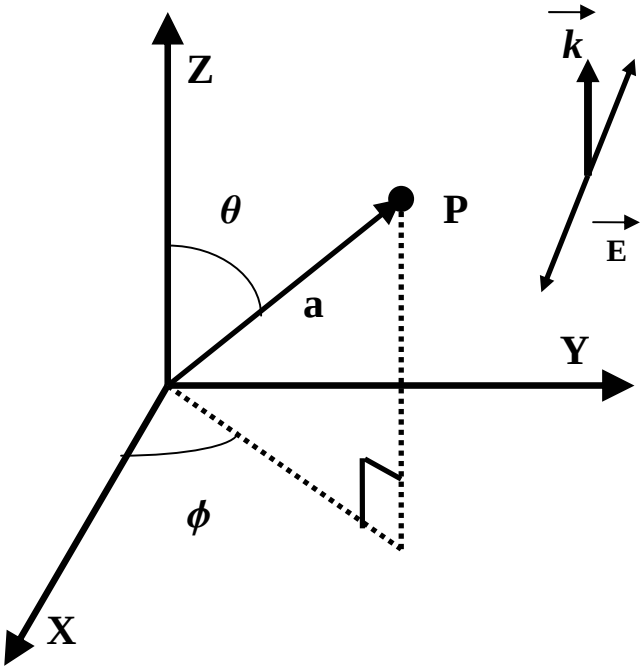

Figure 3.6 Geometry for the numeric calculations

Figure 3.7 (a) and (b) illustrates the geometry for elastic scattering of Gaussian beam from a microsphere. The direction of propagation is in the +Z direction. Figure (a) and (b) shows the accepted TE and TM geometries, respectively. Geometry (a) shows the impact parameter y = -b and θ is scanned from -180^o to 180^o and ϕ = 90^o . Geometry (b) depicts that x = -b , ϕ = 0^o and θ is scanned between -180^o to 180^o.

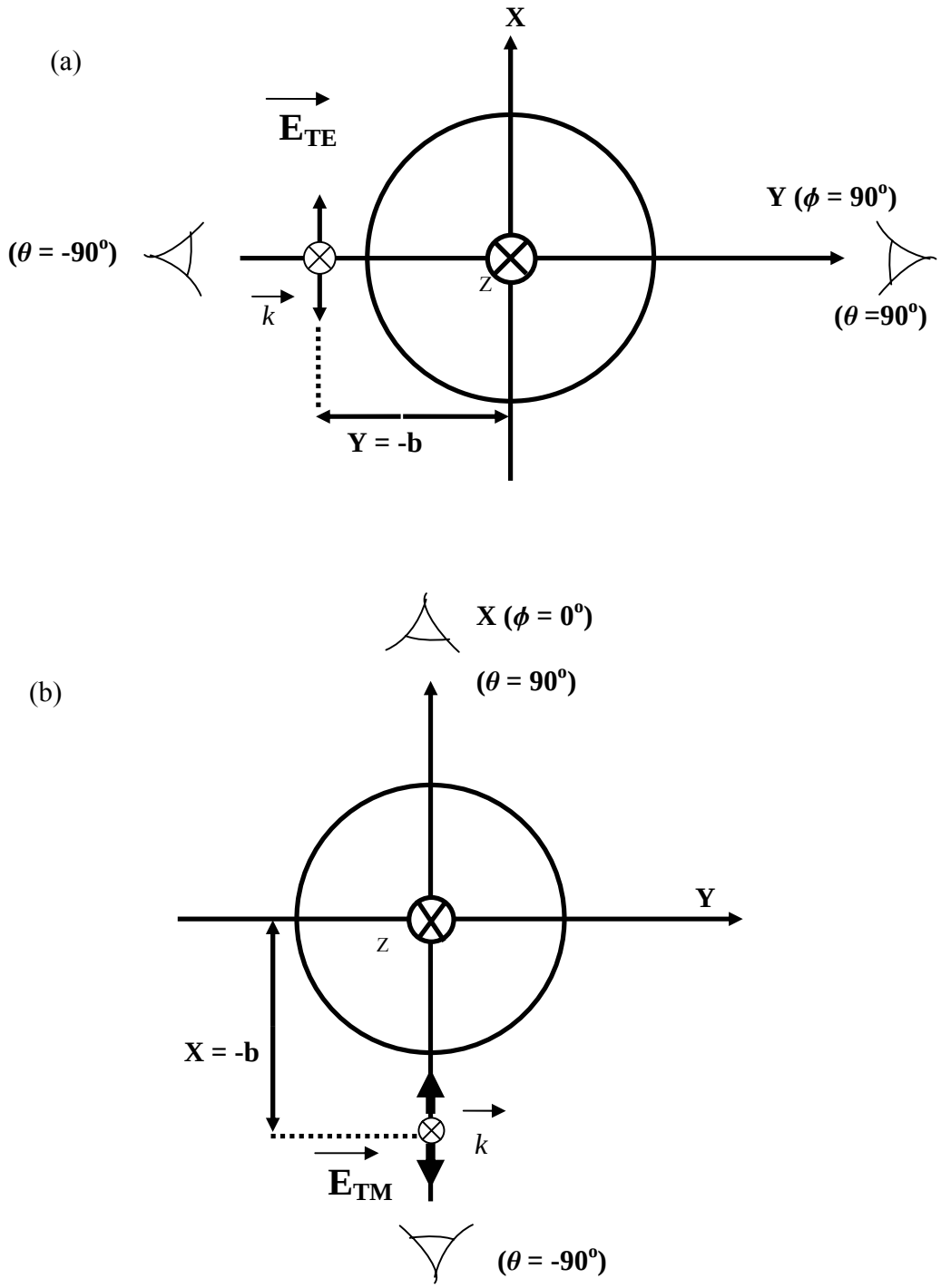

Figure 3.7 Geometry for (a) TE and (b) TM calculations

Chapter 4

RAINBOW ENHANCED SCATTERING IN NEAR-IR WAVELENGTHS

4.1 Introduction

Conventional C-band between 1530 and 1570 nm, is a suitable range for wavelength division multiplexing (WDM) applications, since fiber optic attenuation loss is minimum at 1550 nm. Dense and coarse WDM systems consisting of multiplexers, demultiplexers [36], filters [37], modulators [38] all operate at 1550 nm wavelength [41]. Hence we investigate the elastic scattering properties of microspheres to study the possibility of using microspheres for WDM component applications.

4.2 Calculations and Analysis

In this chapter, the intensity of elastically scattered Gaussian beam from a microsphere is calculated. The wavelength of the beam is scanned between λ = 1530 nm to λ = 1570 nm in the C-band. The radius of the microsphere is a = 10 μm. The half width of the Gaussian beam is ω_0 = 2 μm. The Gaussian beam is impingent on the microsphere with an impact parameter of b = 12 μm. The impact parameter (b = 12 μm) is chosen to maximize the coupling efficiency. The maximum efficiency of coupling to a morphology dependent resonance (MDR) is given in Eq.2.11 and calculated to be 11% at λ = 1550 nm.

Efficient excitation of MDRs requires impact parameters satisfying the equation; ma ⩾ b ⩾ a which corresponds to polar mode numbers satisfying *m*x ⩾ *n* ⩾ x. Intensity calculations are performed for each wavelength and angle pair. The angular resolution of the calculations is 1^o and the wavelength resolution is 0.01 nm.

Figure 4.1 (a) and (b) show the elastic scattering spectra of TE and TM polarized Gaussian beams from the microsphere, respectively. The refractive index of the microsphere is m = 2. For the rainbow order of p = 3, there are three rainbow angles that are -120^o, 0^o, 120^o. Polar mode number (*n*) can take values between 40 and 81. The impact parameter to excite the resonances between polar mode numbers of *n* = 40 and n = 81 is calculated to be between b = 10 μm and 20μm. Therefore our impact parameter b = 12 μm is in the range for exciting morphology dependent resonances (MDR's). The mode spacing between the adjacent mode numbers (*n*) and consecutive mode orders (*l*) is calculated to be Δλ = 23 nm, which agrees well with the estimations.

Figure 4.2 (a) and (b) show the elastic scattering spectra of TE and TM polarized Gaussian beam from the microsphere, respectively. The refractive index of microsphere is m = 1.4142. For a rainbow order of p = 4, there are four rainbow angles that are -90^o, 0^o, 80^o and 180^o. Polar mode number (*n*) can take values between 40 and 57. The impact parameter to excite the resonances between polar mode numbers of *n* = 40 and n = 57 is calculated to be between b = 10 μm and 14.14 μm. Therefore our impact parameter b = 12 μm is in the range for exciting morphology dependent resonances (MDR's). The mode spacing between the adjacent mode numbers (*n*) and consecutive mode orders (*l*) is calculated to be Δλ = 30 nm, which agrees well with the estimations. Lithium Fluoride [40] is a candidate material for applications for this range and refractive index pair.

(a)

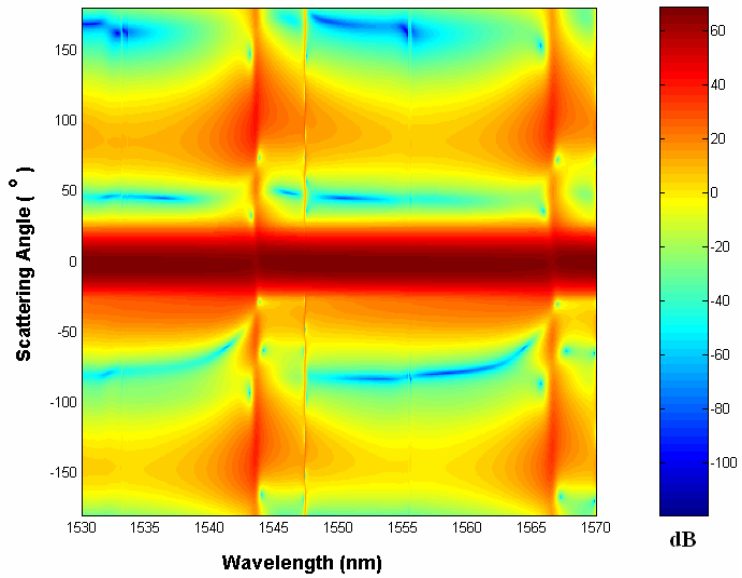

(b)

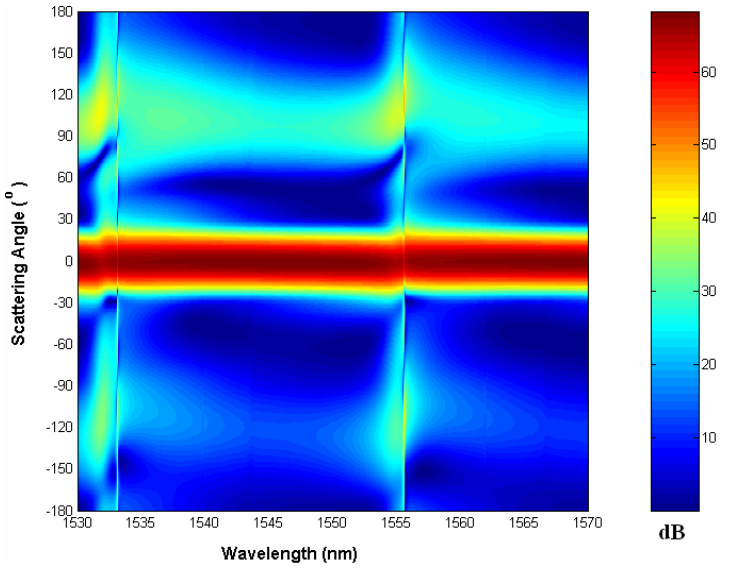

Figure 4.1 False color elastic scattering intensity of (a) transverse electric (TE) (b) transverse magnetic (TM) polarized Gaussian beam from a microsphere of radius a = 10 μm, refractive index m = 2, and rainbow order p =3.

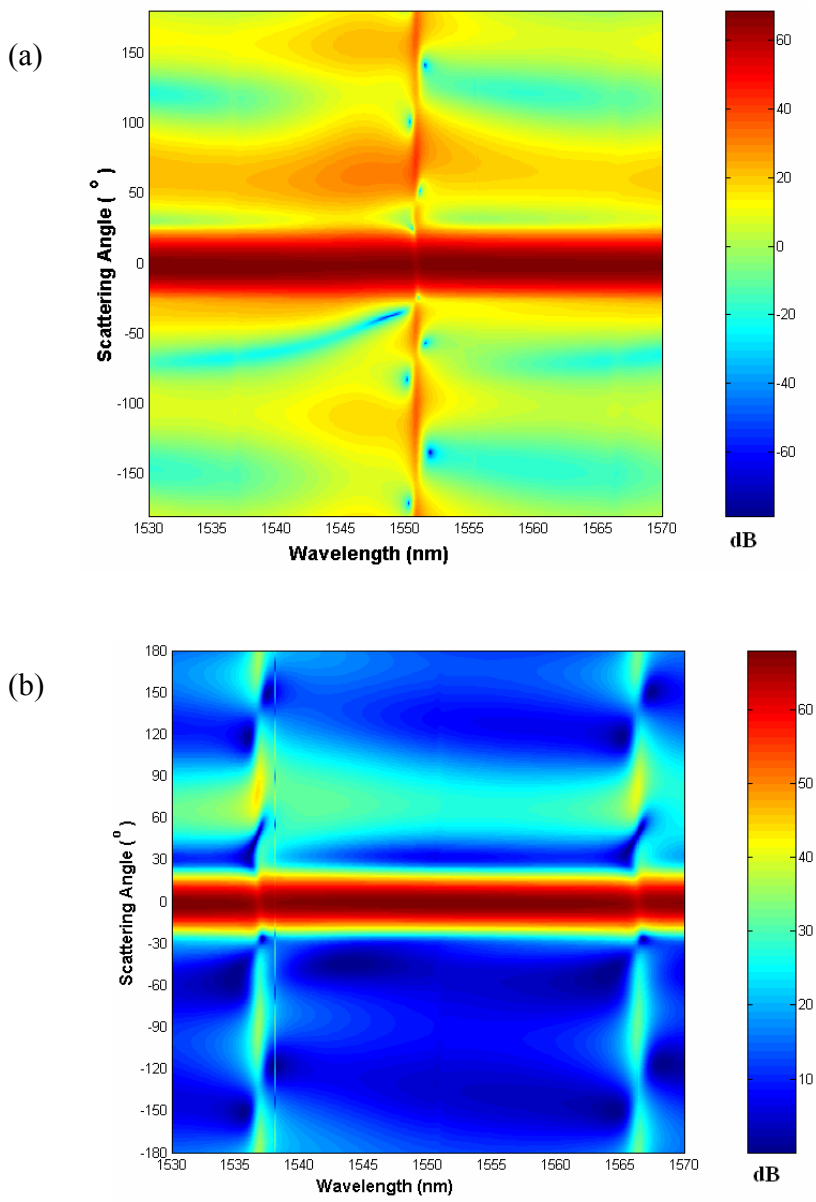

Figure 4.2 False color elastic scattering intensity of (a) transverse electric (TE) (b) transverse magnetic (TM) polarized Gaussian beam from a microsphere of radius a = 10 µm, refractive index m = 1.4142, and rainbow order p =4.

Figure 4.3 (a) and (b) shows the elastic scattering spectra of TE and TM polarized Gaussian beams from the microsphere. The refractive index of the microsphere is m = 1.236. For a rainbow order of p = 5, there are five rainbow angles that are -60^o -150^o, 0^o, 60^o and 150^o. Polar mode number (*n*) can take values between 40 and 50. The impact parameter to excite the resonances between polar mode numbers of *n* = 40 and n = 50 is calculated to be between b = 10 μm and 12.36 μm. The impact parameter of b = 12 μm is in the range for exciting morphology dependent resonances (MDR's). This means the MDR's are enhanced but the interference of MDR and rainbow fields is optimized. The mode spacing between the adjacent mode numbers (*n*) and consecutive mode orders (*l*) is calculated to be $\Delta\lambda$ = 33 nm, which agrees well with the estimations. The elastic scattering intensity is lower with respect to scattering intensity from microspheres with higher refractive indices. The reason is the Q factor. Q factor is proportional to refractive index and as refractive index decreases Q-factor also decreases.

Figure 4.4 (a) and (b) shows the elastic scattering spectra of TE and TM polarized Gaussian beam from the microsphere, respectively. The refractive index of the microsphere is m = 1.15. Polar mode number (*n*) can take values between 40 and 46. The impact parameter to excite the resonances between polar mode numbers of *n* = 40 and n = 46 is calculated to be between b $\cong$ 10 μm and 11.5 μm. The rainbows on the image is not significant. The reason is the low refractive index value (m = 1.15) which decreases the Q-factor and hence scattered field intensity. Another reason is that we used an impact parameter of b = 12 μm. The mode spacing between the adjacent mode numbers (*n*) and consecutive mode orders (*l*) is calculated to be $\Delta\lambda$ = 35 nm, which agrees well with the estimations.

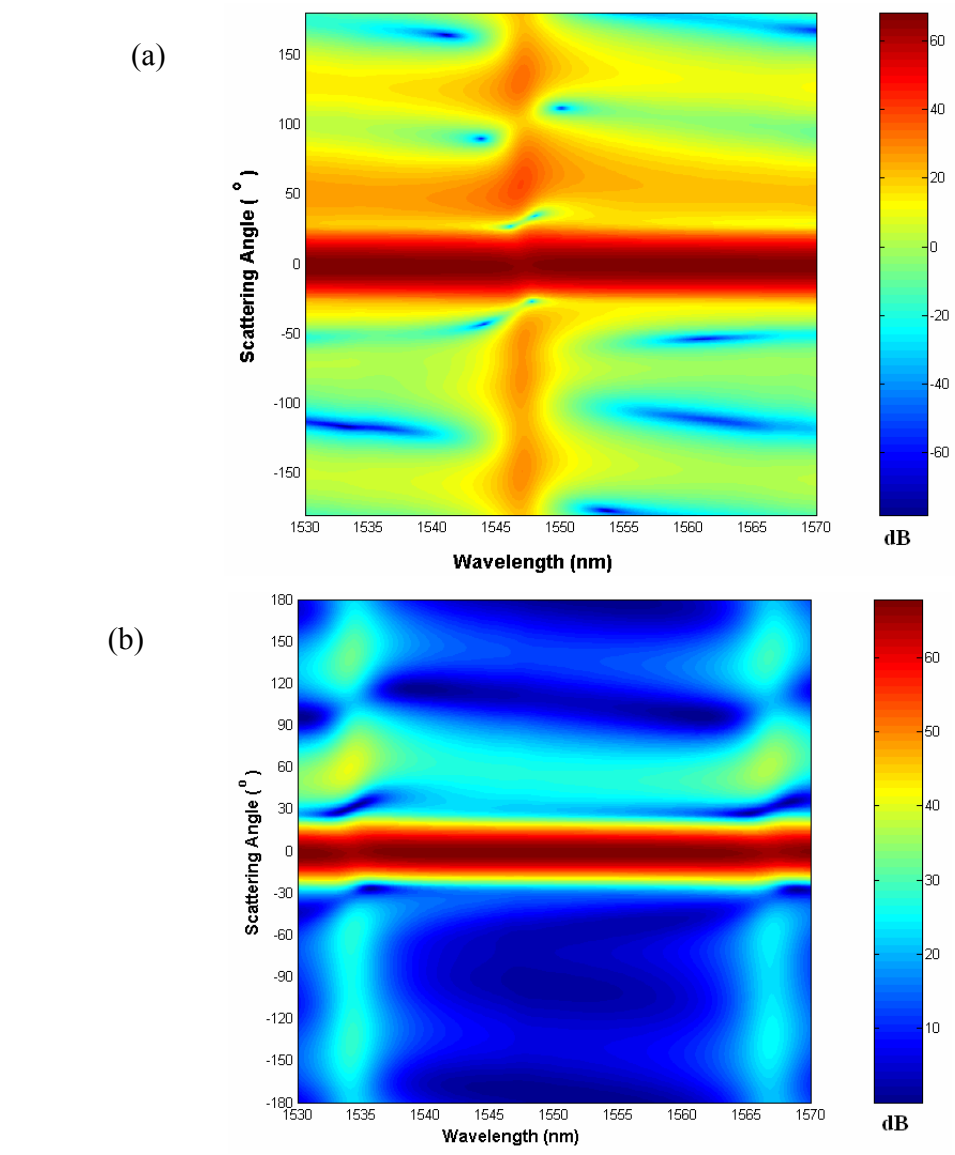

Figure 4.3 False color elastic scattering intensity of (a) transverse electric (TE) (b) transverse magnetic (TM) polarized Gaussian beam from a microsphere of radius a = 10 μm, refractive index m = 1.236, and rainbow order p =5.

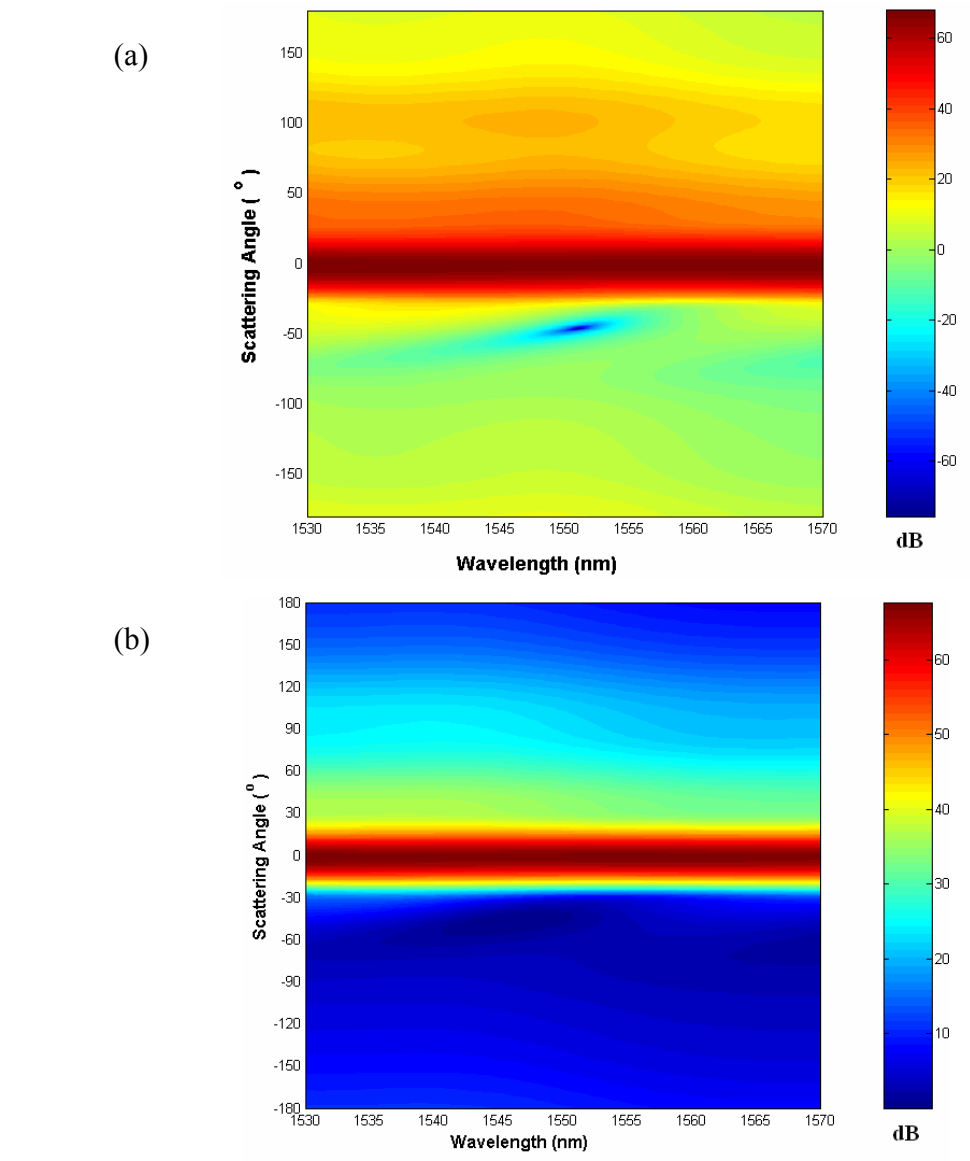

Figure 4.4 False color elastic scattering intensity of (a) transverse electric (TE) (b) transverse magnetic (TM) polarized Gaussian beam from a microsphere of radius a = 10 μm, refractive index m = 1.15, and rainbow order p =6.

.

Chapter 5

RAINBOW ENHANCED SCATTERING IN MID-IR WAVELENGTHS

5.1.Introduction

The developments in communications introduce a congestion problem in standard communication bands between 0.5 MHz and 100 GHz. The congestion between these frequencies and the availability of the communication bandwidth at the mid-IR range make it necessary to design optoelectronic components in the mid-IR region. In the mid-IR region, wavelengths around 10 μm are good candidates for communication due to the fact that atmosphere is transparent at those frequencies. Wavelengths between 10.4 μm and 10.8 μm are considered as the base wavelengths of a mid-IR communication system. A mid-IR optical communication system consists of optical channel dropper [41], optical sources [42], modulators [43], detectors [44], and filters [45].

5.2 Calculations and Analysis

In this chapter, the intensity of elastically scattered Gaussian beam from a microsphere is calculated. The wavelength of the beam is scanned between λ = 10.4 μm to λ = 10.8 μm. The radius of the microsphere is a = 100 μm. The half width of the Gaussian beam is ω_0 = 20 μm. The Gaussian beam is impingent on the microsphere with an impact parameter of b = 120 μm. The impact parameter (b = 120 μm) is chosen to maximize the coupling efficiency. The maximum efficiency of coupling to a morphology dependent resonance (MDR) is given in Eq.2.11 and calculated to be 8% at λ = 10.6 μm. Efficient excitation of MDRs requires impact parameters satisfying the equation; ma $\geqslant$ b $\geqslant$ a which corresponds

to polar mode numbers satisfying mx ⩾ n ⩾ x. Intensity calculations are performed for each wavelength and angle pair. The angular resolution of the calculations is 1^o and the wavelength resolution is 0.2 nm.

Figure 5.1 (a) and (b) show the elastic scattering spectra of TE and TM polarized Gaussian beam from the microsphere, respectively. The refractive index of the microsphere is m = 2. For the rainbow order of p = 3, there are three rainbow angles that are -120^o, 0^o, 120^o. Polar mode number (n) can take values between 59 and 118. The impact parameter to excite the resonances between polar mode numbers of n = 59 and n = 118 is calculated to be between b = 100 μm and 200 μm. Therefore our impact parameter b = 120 μm is in the range for exciting morphology dependent resonances (MDR's). The mode spacing between the adjacent mode numbers (n) and consecutive mode orders (l) is calculated to be $\Delta\lambda$ = 0.108 μm, which agrees well with the estimations.

Figure 5.2 (a) and (b) show the elastic scattering spectra of TE and TM polarized Gaussian beam from the microsphere, respectively. The refractive index of the microsphere is m = 1.4142. For the rainbow order of p = 4, there are four rainbow angles that are 0^o, 80^o, -90^o and 180^o. Polar mode number (n) can take values between 59 and 83. The impact parameter to excite the resonances between polar mode numbers of n = 59 and n = 83 is calculated to be between b = 100 μm and 141 μm. Therefore our impact parameter b = 120 μm is in the range for exciting morphology dependent resonances (MDR's). The mode spacing between the adjacent mode numbers (n) and consecutive mode orders (l) is calculated to be $\Delta\lambda$ = 0.140 μm, which agrees well with the estimations. The candidate material that has m = 2 refractive index value at around 1.55 μm is silicon monoxide (monocrsytalline).

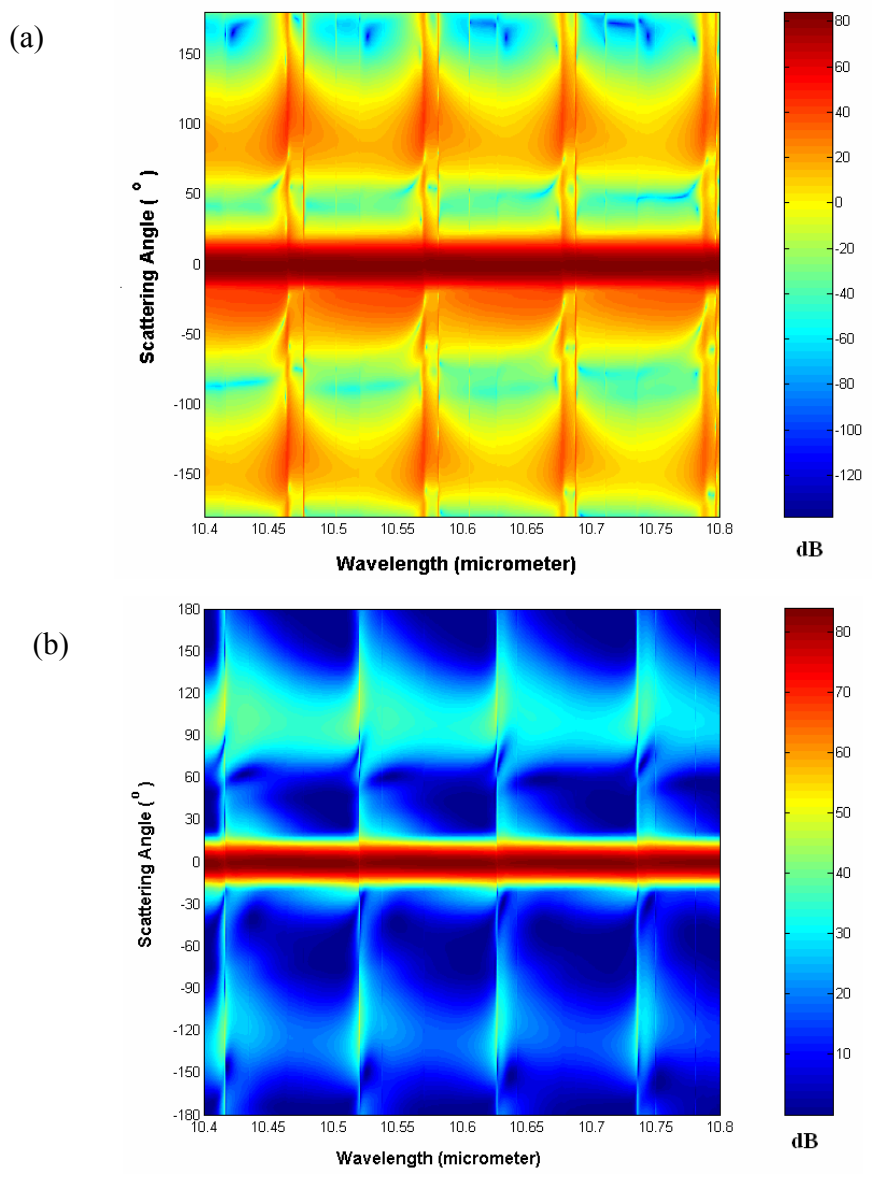

Figure 5.1 False color elastic scattering intensity of (a) transverse electric (TE) (b) transverse magnetic (TM) polarized Gaussian beam from a microsphere of radius a = 100 μm, refractive index m = 2, and rainbow order p =3.

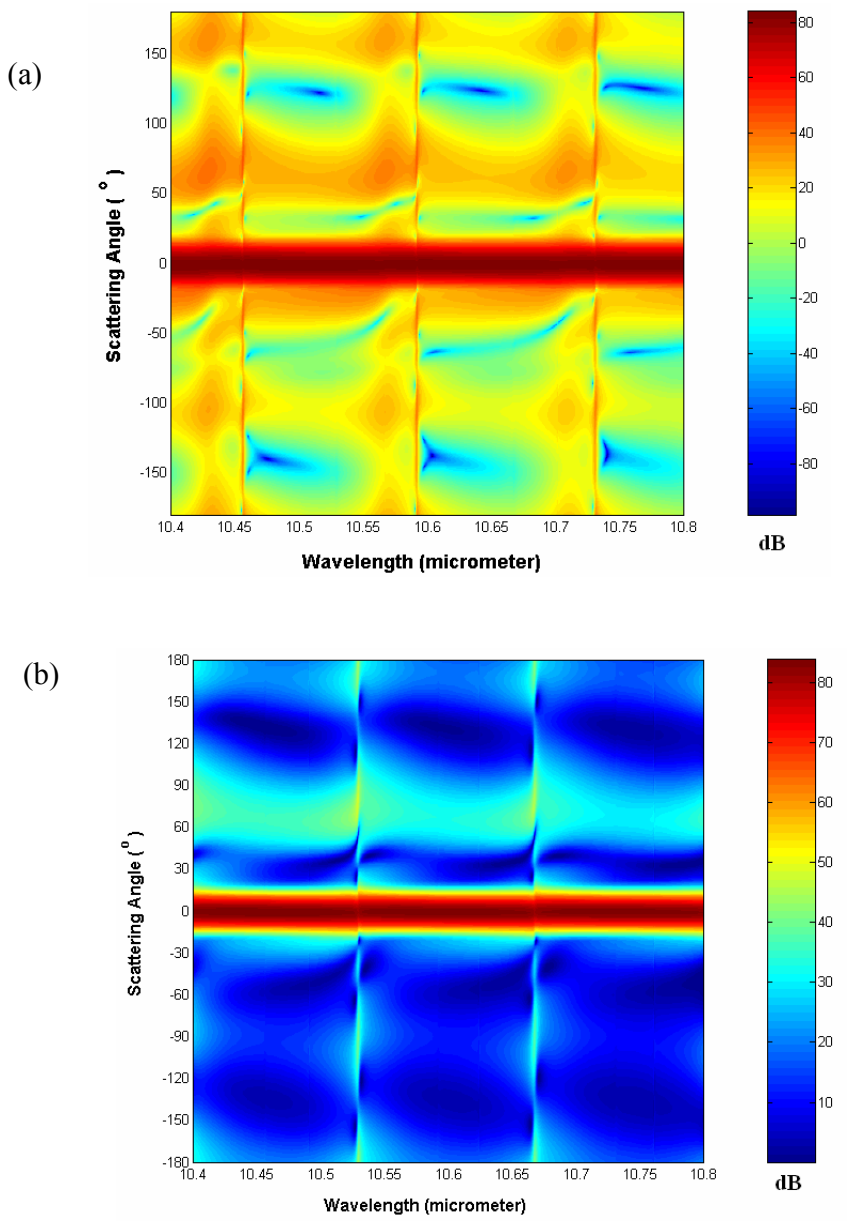

Figure 5.2 False color elastic scattering intensity of (a) transverse electric (TE) (b) transverse magnetic (TM) polarized Gaussian beam from a microsphere of radius a = 100 μm, refractive index m = 1.4142, and rainbow order p =4.

Figure 5.3 (a) and (b) show the elastic scattering spectra of TE and TM polarized Gaussian beam from the microsphere, respectively. The refractive index of the microsphere is m = 1.236. For the rainbow order of p = 5, there are five rainbow angles that are 60^{o}, 0^{o}, 140^{o}, -90^{o}, and -170^{o}. Polar mode number (*n*) can take values between 59 and 73. The impact parameter to excite the resonances between polar mode numbers of *n* = 59 and n = 73 is calculated to be between b = 100 μm and 123.6 μm. Therefore our impact parameter b = 120 μm is in the range for exciting morphology dependent resonances (MDR's). The mode spacing between the adjacent mode numbers (*n*) and consecutive mode orders (*l*) is calculated to be $\Delta\lambda$ = 0.155 μm, which agrees well with the estimations. The candidate material is Lithium Niobate.

Figure 5.4 (a) and (b) show the elastic scattering spectra of TE and TM polarized Gaussian beam from the microsphere, respectively. The refractive index of the microsphere is m = 1.15. For the rainbow order of p = 6, there should be six rainbow angles but they are not observable. Polar mode number (*n*) can take values between 59 and 68. The impact parameter to excite the resonances between polar mode numbers of *n* = 59 and n = 68 is calculated to be between b = 100 μm and 115 μm. Therefore our impact parameter b = 120 μm is not in the range for exciting morphology dependent resonances (MDR's) efficiently. The mode spacing between the adjacent mode numbers (*n*) and consecutive mode orders (*l*) is calculated to be $\Delta\lambda$ = 0.163 μm, which agrees well with the estimations.

(a)

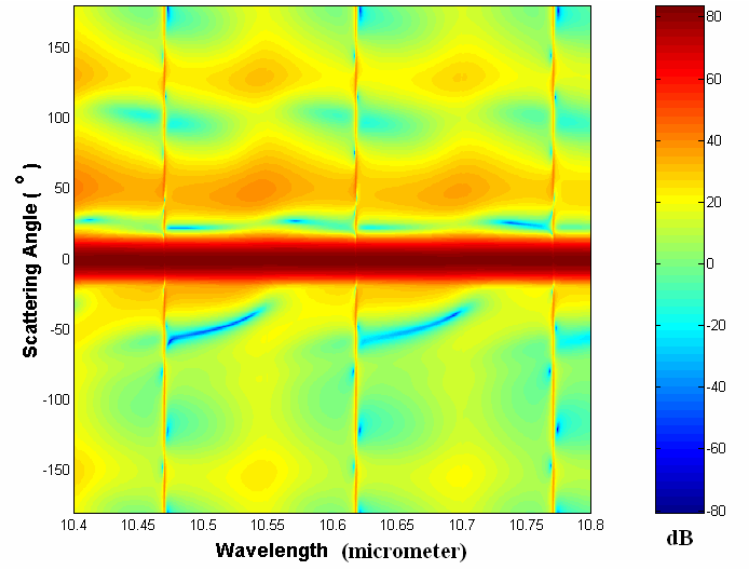

(b)

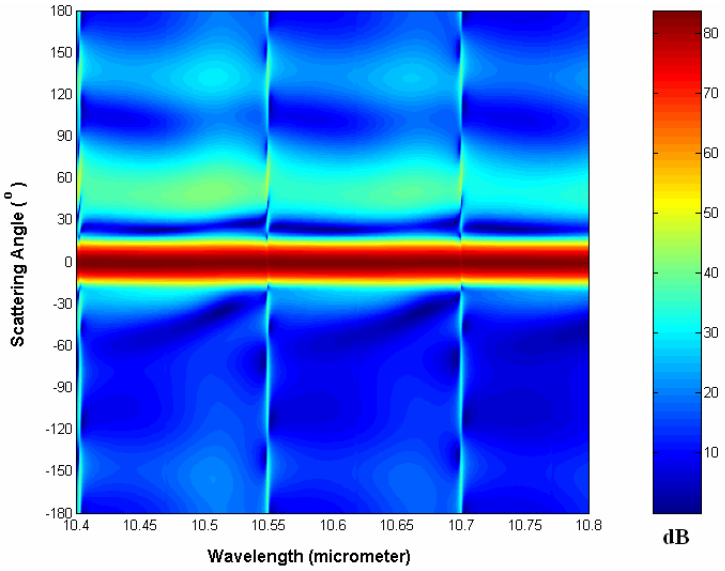

Figure 5.3 False color elastic scattering intensity of (a) transverse electric (TE) (b) transverse magnetic (TM) polarized Gaussian beam from a microsphere of radius a = 100 μm, refractive index m = 1.236, and rainbow order p =5.

(a)

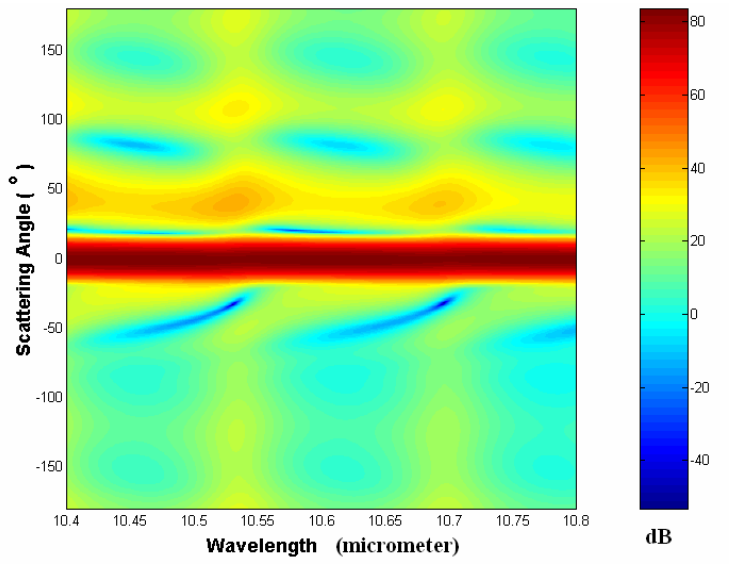

(b)

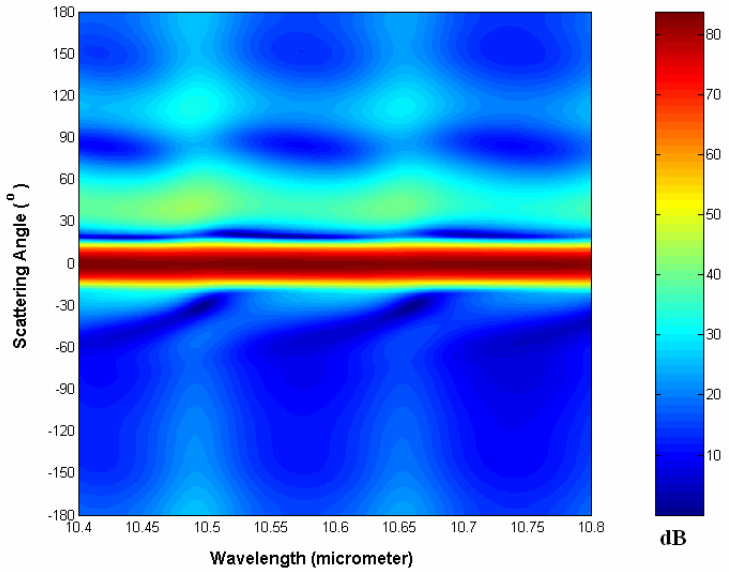

Figure 5.4 False color elastic scattering intensity of (a) transverse electric (TE) (b) transverse magnetic (TM) polarized Gaussian beam from a microsphere of radius a = 100 μm, refractive index m = 1.15, and rainbow order p =6.

Chapter 6

RAINBOW ENHANCED SCATTERING IN FAR-IR WAVELENGTHS

6.1.Introduction

We are searching for new potential communication bands. Far-IR range around 100 μm which is 3 THz in frequency domain is our target investigation wavelength. This wavelength is not appropriate for atmospheric applications due to the fact that atmospheric absorption is high at around 3 THz. There are studies about applications such as photodetectors [46], and lasers[47] to utilize far-IR range for space based communication.

6.2.Calculations and Analysis

We calculate rainbow enhanced elastic scattering intensity from a microsphere of radius a = 500 μm. Beam width of the Gaussian beam is ω_0 = 200 μm. The impact parameter b = 700 μm. Elastic scattering calculations are performed between wavelengths 95-100 μm for refractive indices of m = 2, 1.4241, 1.24, and 1.15. These values correspond to periodic rainbows of n_R = 3, 4, 5, and 6 internal reflections, respectively. The angular resolution of elastic scattering calculations is 1^o. The wavelength resolution of the calculations is 2.5 nm. Calculated excitation efficiency by Eq.2.10 is %7. There are high and low quality factor resonances. High quality factor resonances are sharper and low quality resonances are wider.

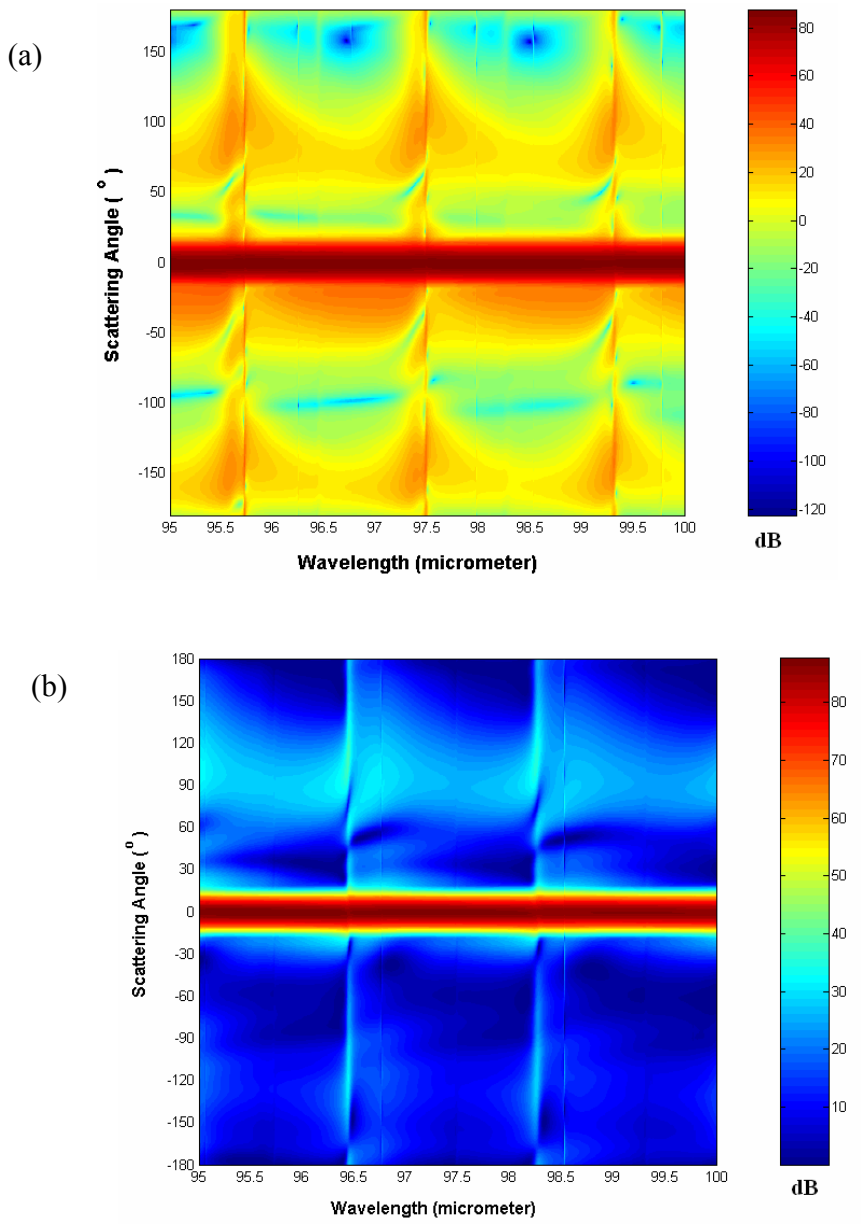

Figure 6.1 False color elastic scattering intensity of (a) transverse electric (TE) (b) transverse magnetic (TM) polarized Gaussian beam from a microsphere of radius a = 500 μm, refractive index m = 2, and rainbow order p =3.

Figure 6.1 (a) and (b) show the elastic scattering spectra of TE and TM polarized Gaussian beam from the microsphere, respectively. The refractive index of the microsphere is m = 2. For the rainbow order of p = 3, there are three rainbow angles that are -120^o, 0^o, 120^o. Polar mode number (*n*) can take values between 32 and 64. The impact parameter to excite the resonances between polar mode numbers of *n* = 32 and n = 64 is calculated to be between b = 500 μm and 1000 μm. Our impact parameter b = 700 μm is in the range for exciting morphology dependent resonances (MDR's). The mode spacing between the adjacent mode numbers (*n*) and consecutive mode orders (*l*) is calculated to be $\Delta\lambda$ = 1.92 μm, which agrees well with the estimations. Candidate material for applications is Lead Telluride.

Figure 6.2 (a) and (b) show the elastic scattering spectra of TE and TM polarized Gaussian beam from the microsphere, respectively. The refractive index of the microsphere is m = 1.4142. For the rainbow order of p = 4, there are four rainbow angles that are 0^o, 150^o, -100 ^{o}, and 90 ^{o} Polar mode number (*n*) can take values between 32 and 45. The impact parameter to excite the resonances between polar mode numbers of *n* = 32 and n = 45 is calculated to be between b = 500 μm and 707 μm. Therefore our impact parameter b = 700 μm is in the range for exciting morphology dependent resonances (MDR's). The mode spacing between the adjacent mode numbers (*n*) and consecutive mode orders (*l*) is calculated to be $\Delta\lambda$ = 2.5 μm, which agrees well with the estimations. Potassium chloride is the material that has refractive index of m = 1.4142 at 100 μm and can be a candidate for various photonic applications.

(a)

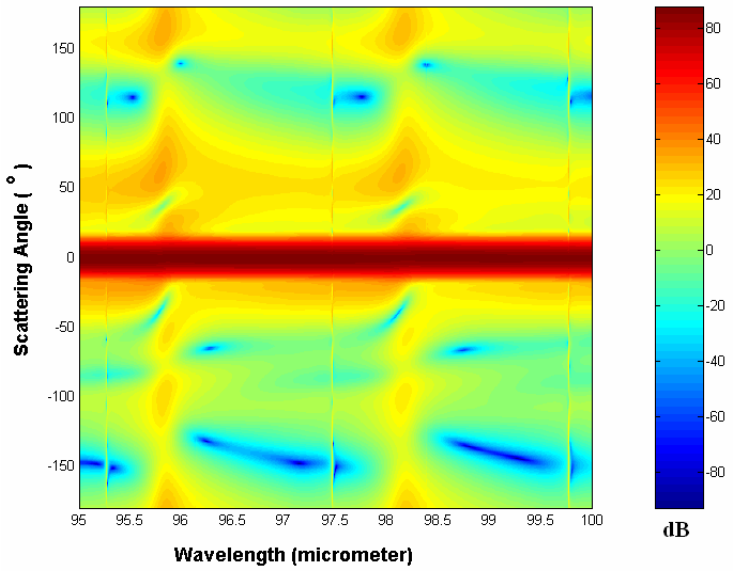

(b)

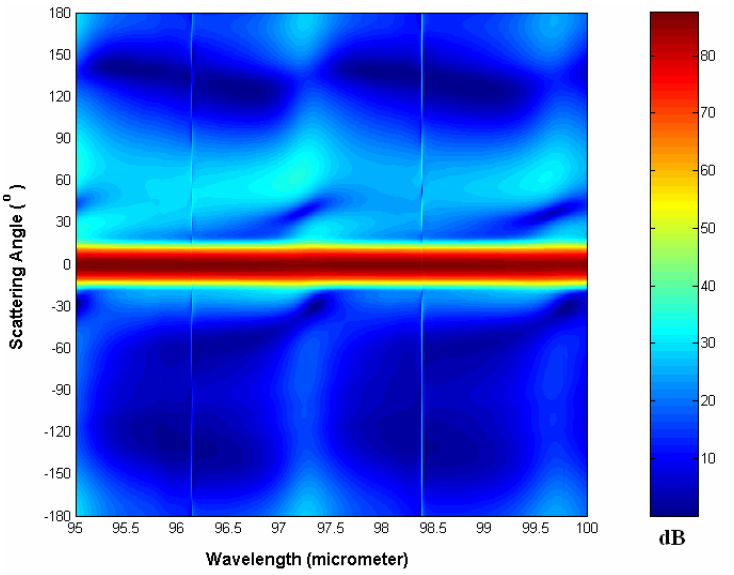

Figure 6.2 False color elastic scattering intensity of (a) transverse electric (TE) (b) transverse magnetic (TM) polarized Gaussian beam from a microsphere of radius a = 500 μm, refractive index m = 1.4142, and rainbow order p =4.

Figure 6.3 (a) and (b) show the elastic scattering spectra of TE and TM polarized Gaussian beam from the microsphere, respectively. The refractive index of the microsphere is m = 1.236. For the rainbow order of p = 5, there are three rainbow angles that are 0 ^{o}, 50^{o}, 150 ^{o}, -160 ^{o} , and -60 ^{o} Polar mode number (*n*) can take values between 32 and 39. The impact parameter to excite the resonances between polar mode numbers of *n* = 32 and n = 39 is calculated to be between b = 500 μm and 620 μm. The mode spacing between the adjacent mode numbers (*n*) and consecutive mode orders (*l*) is calculated to be $\Delta\lambda$ = 2.75 μm, which agrees well with the estimations.

Figure 6.4 (a) and (b) show the elastic scattering spectra of TE and TM polarized Gaussian beam from the microsphere, respectively. The refractive index of the microsphere is m = 1.15. For the rainbow order of p = 6 , we expect to observe six rainbows but the intensity fluctuations on the figure is not significant because of inefficiently excited MDR's. Polar mode number (*n*) can take values between 32 and 36. The impact parameter to excite the resonances between polar mode numbers of *n* = 32 and n = 36 is calculated to be between b = 500 μm and 575 μm. The mode spacing between the adjacent mode numbers (*n*) and consecutive mode orders (*l*) is calculated to be $\Delta\lambda$ = 2.90 μm, which agrees well with the estimations. As the number of polar modes to be excited decreases the Q-factor decreases and hence the coupling scattering intensity. The candidate material for potential applications is lead selenide.

(a)

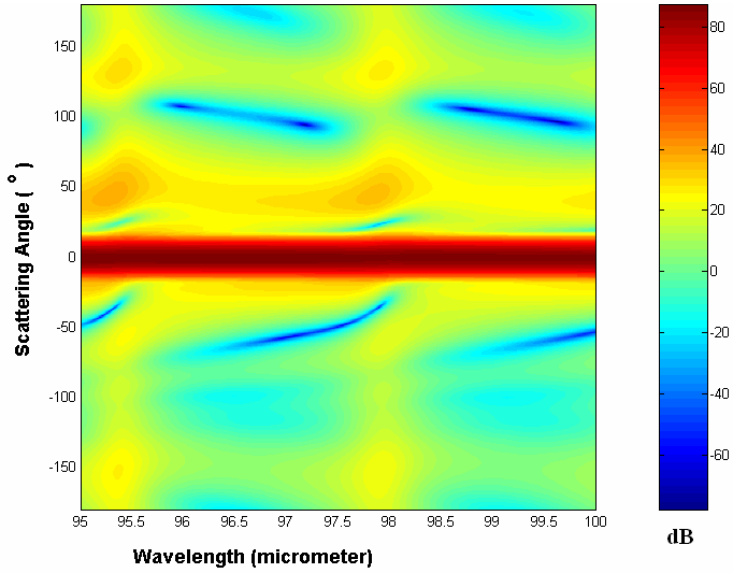

(b)

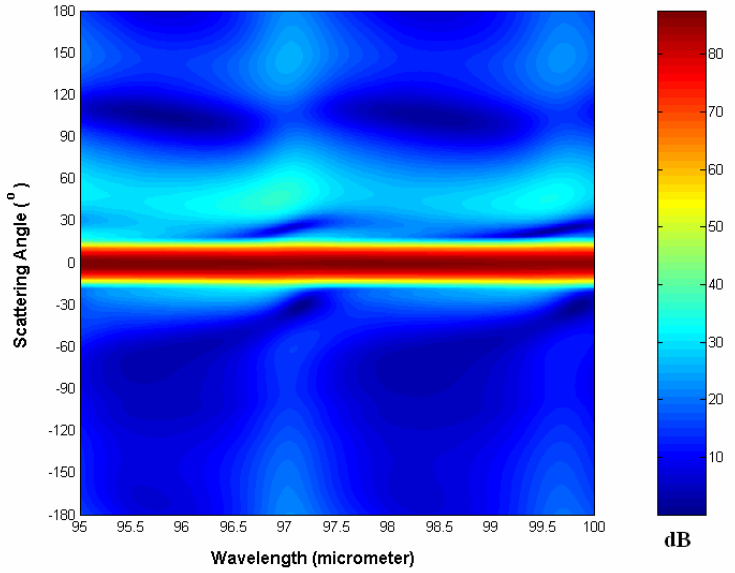

Figure 6.3 False color elastic scattering intensity of (a) transverse electric (TE) (b) transverse magnetic (TM) polarized Gaussian beam from a microsphere of radius a = 500 μm, refractive index m = 1.236, and rainbow order p =5.

(a)

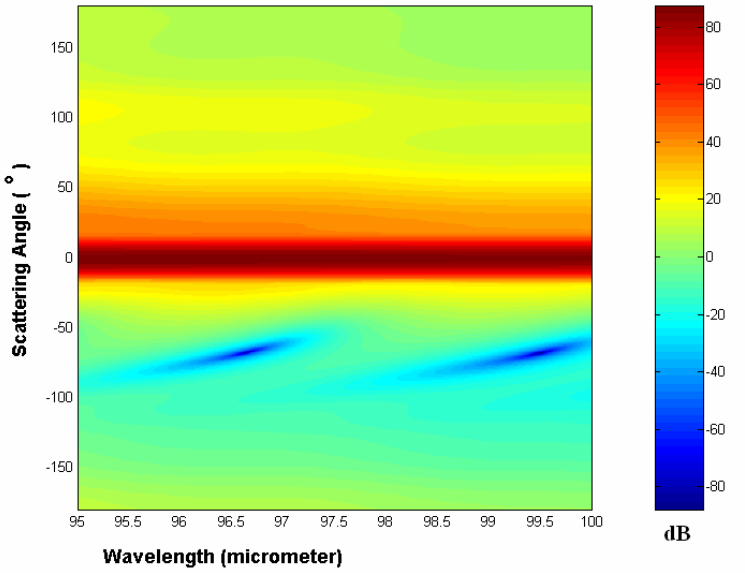

(b)

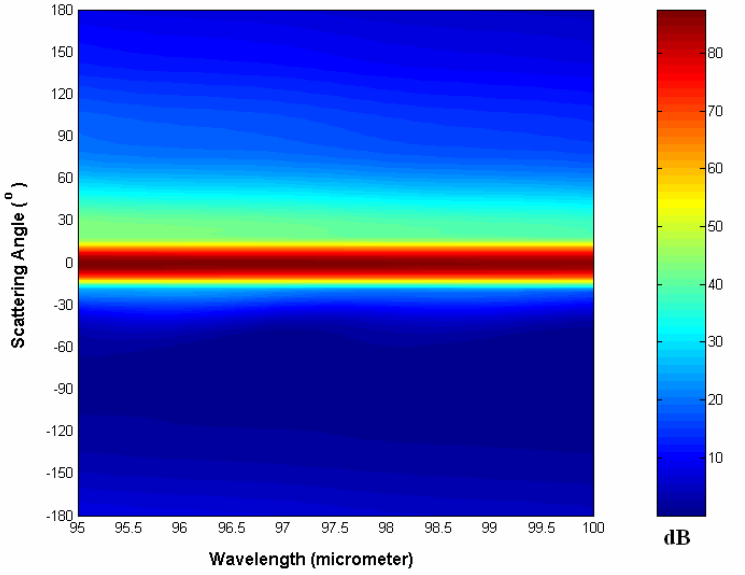

Figure 6.4 False color elastic scattering intensity of (a) transverse electric (TE) (b) transverse magnetic (TM) polarized Gaussian beam from a microsphere of radius a = 500 μm, refractive index m = 1.15, and rainbow order p = 6.

CONCLUSION

In this thesis we have concentrated on the elastic scattering properties of off-axis focused Gaussian beams in order to investigate the application of microspheres for optical communication. Three infrared bands are studied.

First, near-IR, the conventional C-band is chosen because of its widely used in WDM applications due to the fact that attenuation loss is very low. We have calculated elastic scattering for refractive indices of m = 2, 1.4142, 1.236, and 1.15, and investigated whether there is scattering enhancement due to rainbow formation. Enhancement depends on relative phase of MDR and rainbow and is a very sensitive function of size parameter. The maximum coupling efficiency in that range provided that apropriate impact parameters are chosen is % 11. Candidate materials for near infrared applications are lithium flouride for m = 1.4142.

Secondly mid-IR range is studied for wavelengths between 10.4 μm and 10.8μm. This range is suitable for atmospheric applications because atmospheric absorption is very low around 10 μm. Maximum efficiency of coupling is calculated to be %8. Candidate materials for m = 2 and m = 1.236 are Monocrystalline Silicon Monoxide and Lithium Niobate, respectively.

Finally we studied elastic scattering from spheres at wavelengths between 95 μm and 100μm. Excitation efficiency (coupling efficiency) of MDRs is calculated to be %7. Candidate materials for refractive indices are lead telluride for m = 2 , potassium chloride for m =1.4142 and lead selenide for m = 1.15

As a conclusion, we have studied the effect of the rainbows on the MDRs. The enhancement depends on the size parameter, refractive index, and the impact parameter.

The excitation efficiencies that are calculated are maximum values. In order to achieve these values, impact parameters should be chosen for maximum efficiency by determining the polar mode numbers (*n*). We have calculated elastic scattering properties of microspheres for certain refractive indices and wavelengths. Additionally we found candidate materials that can be used for the calculated refractive index, wavelength pairs.

BIBLIOGRAPHY

[1] C. A. Barios, V. R. Almeida, R. R. Panepucci, B. S. Schmidt, and M. Lipson," Compact Silicon Tunable Fabry-Perot Resonator With Low Power Consumption" IEEE Photon. Technol. Lett., 16, 506-508 (2004)

[2] A. J. Cox and D. C. Dibble, "Nondiffracting beam from a spatially filtered Fabry-Perot resonator," J. Opt. Soc. Am. A 9, 282 (1992)

[3] P Rabiei, WH Steier, C Zhang, and LR Dalton "Polymer Micro-Ring Filters and Modulators", Journal of Lightwave Technol., 20, 1968 (2002)

[4] V.S. Ilchenko, P.S. Volikov , V.L. Velichansky , F. Treussart, V. Lefevre-Seguin , J. M. Raimond, S. Haroche, " Strain-tunable high-Q optical microsphere resonator" Optics Communication, 145, 1, 86-90 (1998)

[5] K. Vahala, Ed., Optical Microcavities, World Scientific, Singapore, (2004).

[6] K. J. Vahala, "Optical Microcavities", Nature 424, 839-846 (2003).

[7] A. A. Savchenkov, V. S. Ilchenko, A. B. Matsko, and L. Maleki, "Kilohertz optical resonances in dielectric crystal cavities", Phys. Rev. A 70, 051804(R) (2004).

[8] M. Cai, G. Hunziker, and K. Vahala, "Fiber optic add-drop device based on a silica microsphere-whispering gallery mode system," IEEE Photon. Technol. Lett. 11, 686-687 (1999).

[9] H.C. Tapalian, J.P. Laine, and P.A. Lane, "Thermooptical switches using coated microsphere resonators," IEEE Photon. Technol. Lett. 14, 1118-1120, (2002).

[10] I. Teraoka, S. Arnold, and F. Vollmer, "Perturbation approach to resonance shifts of whispering-gallery modes in a dielectric microsphere as a probe of a surrounding medium," J. Opt. Soc. Am. B, 20, 1937-1946, (2003).

[11] J. P. Laine, H. C. Tapalian, B. E. Little, and H. A. Haus, "Acceleration sensor based on high-Q optical microsphere resonator and pedestal antiresonant reflecting waveguide coupler," Sensors and Actuators A, 93, 1-7 (2001).

[12] A.B. Matsko, A.A. Savchenkov, V.S. Ilchenko, and L. Maleki, “Optical gyroscope with whispering gallery mode optical cavities,” Opt. Commun., 233, 107–112 (2004).

[13] J. A. Lock “ An improved gaussian beam scattering algorithm,” Appl. Opt. 34, 559 (1995)

[14] L. Rayleigh, “The problem of the whispering gallery,” Scientific Papers 5, 617 (1912).

[15] V. Sandoghdar, F. Treussart, J. Hare, V. Lefevre-Seguin, J. M. Raimond, and S. Haroche, “Very Low Threshold Whispering-gallery-mode Microsphere Laser”, Physical Review A, 54, 3, (1996)

[16] J. P. Laine, B. E. Little, and H. A. Haus, “Etch-Eroded Fiber Coupler for Whispering-gallery-mode Excitation in High Q Silica Microspheres”, IEEE Photonics Technology Letters, 11, 11, (1999).

[17] M. Pelton and Y.Yamamoto, “Ultralow Threshold Laser Using a Single Quantum Dot and a Microsphere Cavity”, Physical Review A, 59, 3, (1999).

[18] B. R. Johnson, “Morphology Dependent Resonances of a Dielectric Sphere on a Conducting Plane”, J. Opt. Soc. Am. A, 11, 7, 2055-2064, (1994).

[19] L. G. Guimardes and H. M. Nussenzveig, “Theory of Mie resonances and ripple fluctuations,” Opt. Commun. 89, 363-369 (1992).

[20] G. Mie, “Beiträge zur Optik trüber Medien, speziell kolloidaler Metallösungen,” Ann. Phys. Leipzig 25, 377–445 (1908).

[21] E. Wolf, Ed., Progress in Optics, 41, Elsevier, Netherlands (2000).

[22] Barber P. W., and S. C. Hill, Eds., Light Scattering by Particles: Computational Methods, World Scientific, Singapore (1990).

[23] C. F. Bohren and D. R. Huffman, Absorption and Scattering of Light by Small Particles, Interscience, New York (1983).

[24] Gurvich I., N. Shiloah, and M. Kleiman, “Calculations of The Mie Scattering Coefficients for Multilayered Particles with Large Size Parameters”, Journal of Quantitative Spectroscopy & Radiative Transfer, 70, 433-440, (2001).

[25] Barton J. P., D. R. Alexander, and S. A. Schaub, “Internal Fields of a Spherical Particle Illuminated by a Tightly Focused Laser Beam: Focal Point Positioning Effects at Resonance, Journal of Applied Physics, 65, 8, (1989).

[26] Klitzing von W., R. Long, V. S. Ilchenko, J. Hare, and V. Lefevre-Seguin, “Tunable Whispering Gallery Modes for Spectroscopy and CQED Experiments”, New Journal of Physics, 3, 14.1-14.14, (2001).

[27] Guillon P. and Y. Garault, “Accurate Resonant Frequencies of Dielectric Resonators”, IEEE Transactions on Microwave Theory and Techniques, MTT-25, 11, 916-922, (1977).

[28] Laine J.-P., C. Tapalian, B. Little, H. Haus, “Acceleration Sensor Based on High-Q Optical Microsphere Resonator and Pedestal Antiresonant Reflecting waveguide Coupler”, Sensors and Acutators A, 93, 1-7, (2001).

[29] B. E. Little, J. P. Laine, and H. A. Haus, “Analytic theory of coupling from tapered fibers and half-blocks into microsphere resonators.” Journal of Lightwave Technology 17, 704-715, (1999)

[30] A. Serpengüzel, S. Arnold, G. Griffel, J. A. Lock “ Enhanced coupling to microsphere resonances with optical fibers” J. Opt. Soc. Am. B, 14 4, 790-795, (1997)

[31] S. A. Schaub, J. P. Barton, and D. R. Alexander, “Simplified scattering coefficient expressions for a spherical particle located on the propagation axis of a fifth-order Gaussian beam,” Appl. Phys. Lett. 55, 2709-2711(1989).

[32] S. A. Schaub, J. P. Barton and D. R. Alexander, “Simplified scattering coefficient expressions for a spherical particle located on the propagation axis of a fifth-order Gaussian beam,” Appl. Phys Lett. 55, 2709-2711 (1989).

[33] J. P. Barton and D. R. Alexander, “Fifth-order corrected electromagnetic field components for a fundamental Gaussian beam,” J. Appl. Phys. 66, 2800-2802 (1989).

[34] A. Demir " Elastic Scattering of Gaussian Beams from Microspheres" MSc. Thesis Computer Science and Engineering, Koc University, Istanbul, Turkey (2005).

[35] W. T. Grandy, " Scattering of Waves from Large Spheres" Cambridge University Press, Edinburg, (2000)

[36] F. Bilodeau, D. C. Johnson, S. Theriault, B. Malo," An All-Fiber Dense-Wavelength-Division Multiplexer/Demultiplexer Using Photoimprinted Bragg Gratings" IEEE Photonic Technol. Lett., 7, 388 (1995)

[37] J. B. D. Soole,. M.R. Amersfoort, H. P. LeBlanc, N. C. Andreadakis, A. Rajhel, C. Caneau, R. Bhat, M. A. Koza, C. Youtsey, I. Adesida," Use of Multimode Interference Couplers to Broaden the Passband of Wavelength-Dispersive Integrated WDM Filters" IEEE Photonic Technol. Lett., 8, 1340-1342 (1996)

[38] L. Y. Chan, C. K. Chan, D. T. K. Tong, F. Tong, L. K. Chen," Upstream traffic transmitter using injection-locked Fabry-Perot laser diode as modulator for WDM access networks" IEE Electronics Lett., 38, 43-44 (2002)

[39] S. Aisawa, T. Sakamoto, M. Fukui, J. Kani, M. Jinno, K. Oguchi" Ultra-wideband, long distance WDM demonstration of 1 Tbit/s (50 × 20 Gbit/s), 600 km transmission using 1550 and 1580 nm wavelength bands" Electronic Lett., 34, 1127-1129 (1998)

[40] E. D. Palik "Handbook of optical constants of Solids" Academic Pres, California, (1985)

[41] Y. O. Yilmaz, A. Demir, A. Kurt and A. Serpengüzel, " Optical Channel Dropping with a Silicon Microsphere", IEEE Photonic Technol. Lett., 17, 1662-1664, (2005).

[42] R. Koehler, A. Tredicucci, F. Beltram, H. E. Beere, H. E. Linfield, A. G. Davies, D. A. Ritchie, S. S. Dhillon, C. Sirtori, "High-Performance Continuous-Wave Operation of Superlattice THz Quantum Cascade Lasers", Appl. Phys. Lett. 82, 1518-1520, (2003).

[43] M. Y. Su, S. Carter, M. S. Sherwin, A. Huntingdon and L. A. Coldren, "Voltage Controlled Wavelength Conversion by THz Electro-Optic Modulation in Double Quantum Wells", Appl. Phys. Lett. 81, 1564-1566, (2002).

[44] F. Klappenberger, A. A. Ignatov, S. Winnerl, E. Schomburg, W. Wegscheider and K. F. Renk, “Broadband Semiconductor Superlattice Detector for THz Radiation” , Appl. Phys. Lett. 78, 1673-1675 (2001).

[45] I. H. Libon, S. Baumgartner, M. Hempel, N. E. Hecker and J. Feldman, M. Koch and P. Dawson,“An Optically Controllable THz Filter,“ Appl. Phys. Lett. 76, 2821-2823, (2000).

[46] N. Hiromoto, H. Fujiwarai “Slow transient response of Ge:Ga far-infrared photoconductors for space applications” Infrared Physics and Technology, 40, 387-393 (1999).

[47] G. Dogel “On the history of far-infrared (FIR) gas lasers: Thirty-five years of research and application” Infrared Physics and Technology, 40, 127-139 (1999).

VITA

Onur Akatlar graduated from Ümraniye Anatolian High School in Istanbul in 1999. He graduated from Bogazici University, Physics Department in Istanbul in 2004. He worked on numerical calculations on the accumulation of cylindrical particles as an independent research in Bogazici University. He joined the M.S.c. program on Material Science and Engineering in Koç University in 2004 and worked in Koç University Microphotonics Research Laboratory for two years. He worked on elastic scattering of plane waves and Gaussian beams from microspheres. Additionally, he worked on Stimulated Raman scattering from silicon microspheres. He has been a teaching and research assistant, since he joined Koç University.